



Amarillo National Resource Center for Plutonium

A Higher Education Consortium of The Texas A&M University System,
Texas Tech University, and The University of Texas System

Disposition of Weapons-Grade Plutonium in Westinghouse Reactors

March 1998

This report was prepared with the support of the U.S. Department of Energy (DOE) Cooperative Agreement No. DE-FC04-95AL85832. However, any opinions, findings, conclusions, or recommendations expressed herein are those of the author(s) and do not necessarily reflect the views of DOE. This work was conducted through the Amarillo National Resource Center for Plutonium.

600 South Tyler • Suite 800 • Amarillo, TX 79101
(806) 376-5533 • Fax: (806) 376-5561
<http://www.pu.org>

ANRCP-1998-1

**DISPOSITION OF WEAPONS-GRADE PLUTONIUM
IN WESTINGHOUSE REACTORS**

Abdelhalim Ali Alsaed

Texas A&M University
College Station, Texas

Marvin Adams

Texas A&M University
College Station, Texas

Submitted for publication to the

Amarillo National Resource Center for Plutonium

March 1998

ABSTRACT

Disposition of Weapons-Grade Plutonium in Westinghouse Reactors

Abdelhalim Ali Alsaed and Marvin Adams

We have studied the feasibility of using weapons-grade plutonium in the form of mixed-oxide (MOX) fuel in existing Westinghouse reactors. We have designed three transition cycles from an all LEU core to a partial MOX core. We found that four-loop Westinghouse reactors such as the Vogtle power plant are capable of handling up to 45 percent weapons-grade MOX loading without any modifications. We have also designed two kinds of weapons-grade MOX assemblies with three enrichments per assembly and four total enrichments. Wet annular burnable absorber (WABA) rods were used in all the MOX feed assemblies, some burned MOX assemblies, and some LEU feed assemblies. Integral fuel burnable absorber (IFBA) was used in the rest of the LEU feed assemblies. The average discharge burnup of MOX assemblies was over 47,000 MWD/MTM, which is more than enough to meet the “spent fuel standard.” One unit is capable of consuming 0.462 MT of weapons-grade plutonium per year. Preliminary analyses showed that important reactor physics parameters for the three transitions cycles are comparable to those of LEU cores including boron levels, reactivity coefficients, peaking factors, and shutdown margins. Further transient analyses will need to be performed.

ACKNOWLEDGMENTS

I would like to thank Dr. Marvin Adams, my advisor and committee chair, for his extraordinary support and tutelage throughout this project. I would also like to thank Mr. Rick Ankney, my supervisor at Westinghouse, for his exceptional supervision and technical guidance. I would like to extend my gratitude to Dr. Theodore Parish and Dr. Dick Simmons, my committee members. Dr. John Poston deserves acclamation for his auspicious leadership of the Department of Nuclear Engineering, giving me the opportunity to do research that I enjoy and the resources to do it well.

This thesis was prepared with the support of the U.S. Department of Energy (DOE), Cooperative Agreement No. DE-FC04-95AL85832. However, any opinions, findings, conclusions, or recommendations expressed herein are those of the author(s) and do not necessarily reflect the views of DOE. This work was conducted through the Amarillo National Resource Center for Plutonium.

TABLE OF CONTENTS

	Page
ABSTRACT	iii
ACKNOWLEDGMENTS	iv
TABLE OF CONTENTS	v
LIST OF FIGURES.....	vi
LIST OF TABLES	viii
CHAPTER	
I INTRODUCTION	1
II ANALYSIS TOOLS AND DESIGN METHODOLOGY	7
Design Process	7
Analysis Tools	8
Design Methodology.....	9
III WITHIN ASSEMBLY ENRICHMENT OPTIMIZATION	13
IV TRANSITION CYCLES DESIGN AND ANALYSIS	25
First Transition Cycle.....	25
Second Transition Cycle	35
Third Transition Cycle	40
Analysis of Transition Cycles	45
Summary	57
V SUMMARY AND CONCLUSIONS.....	59
REFERENCES.....	63
VITA.....	65

LIST OF FIGURES

FIGURE		Page
1	Schematic of a colorset	8
2	One-dimensional representation of assumed global power effect....	10
3	Engineering judgment based preliminary design of first transition cycle	14
4	Quadrants of a MOX-LEU colorset	17
5	Pin-peaking as a function of burnup in a MOX-LEU colorset with zoned and flat MOX assemblies	18
6	Effect of simulated global power shape on pin-peaking	19
7	Final design of the first transition cycle	20
8	MOX assembly with 4.515 w/o Pu-fissile average enrichment	22
9	MOX assembly with 3.992 w/o Pu-fissile average enrichment	23
10	Effect of zoned MOX assemblies on pin-peaking in a partial-MOX core	24
11	Step-by-step design of a transition cycle.....	29
12	Final design of the first transition cycle	30
13	Layout of assembly average power, radial pin-peaking, and assembly average burnup at BOC (150 MWD/MTM).....	32
14	Layout of assembly average power, radial pin-peaking, and assembly average burnup at MOC (11,000 MWD/MTM)	33
15	Layout of assembly average power, radial pin-peaking, and assembly average burnup at EOC (21,564 MWD/MTM)	34
16	Final design of the second transition cycle.....	36

FIGURE		Page
17	Layout of assembly average power, radial pin-peaking, and assembly average burnup at BOC (150 MWD/MTM).....	37
18	Layout of assembly average power, radial pin-peaking, and assembly average burnup at MOC (11,000 MWD/MTM)	38
19	Layout of assembly average power, radial pin-peaking, and assembly average burnup at EOC (21,564 MWD/MTM)	39
20	Final design of the third transition cycle	41
21	Layout of assembly average power, radial pin-peaking, and assembly average burnup at BOC (150 MWD/MTM).....	42
22	Layout of assembly average power, radial pin-peaking, and assembly average burnup at MOC (11,000 MWD/MTM)	43
23	Layout of assembly average power, radial pin-peaking, and assembly average burnup at EOC (21,564 MWD/MTM)	44
24	HFP critical boron letdown curves	47
25	Post LB-LOCA boron concentration as a function of pre-LBLOCA boron concentration.	49
26	HFP boron coefficient versus burnup	50
27	HFP MTC as a function of burnup	51
28	BOC TPC versus power	52
29	EOC TPC versus power	53
30	HFP radial pin-peaking versus burnup.....	54
31	HFP local power peaking versus burnup	55

LIST OF TABLES

TABLES		Page
I	Depleted Uranium Isotopics.....	5
II	Weapons-Grade and Reactor-Grade Plutonium Isotopics	5
III	Vogtle Specific Operating and Design Parameters.....	26
IV	Thermal and Resonance-Integral Cross Sections for U-235 and Pu-239.....	27
V	Neutron Spectra Comparison.....	45
VI	Burnable Absorber Loading Comparison.....	46
VII	Critical Boron Concentration Comparison.....	48
VIII	MTC Comparison at BOC, HZP, No Xenon Conditions	50
IX	EOC SDM Calculations	57
X	Summary of Design Parameters	61

CHAPTER I

INTRODUCTION

The road to world peace is likely to be surrounded by compromises and paved with sacrifices. Most people agree that control, containment and reduction of mass-destruction weapons is an important step down that road. In recent years, negotiations between the United States (US) and the Newly Independent States of the Former Soviet Union (NISFSU) have resulted in agreements to reduce nuclear weapons stockpiles. On its part, within the next decade, the US will dismantle enough nuclear weapons to produce a surplus of 38.2 metric tons (MT) of weapons-grade plutonium (WGPu)¹. The existence of this surplus of WGPu poses many dangers including the potential of nuclear weapons proliferation as well as environmentally harmful releases.²

The National Academy of Sciences (NAS) Committee on International Security and Arms Control (CISAC) conducted a study² on management and disposition of excess WGPu upon a request from the US Secretary of Energy. NAS expects that a total of 38.2 MT of WGPu, along with a few hundred MT of highly enriched uranium (HEU), will be surplus within the next decade. Even though the amount of HEU greatly exceeds the surplus of WGPu, it is considered manageable. HEU can easily be mixed with natural or depleted uranium to produce low-enriched uranium (LEU) fuel which is used in most of the world's light-water reactors (LWRs). The cost of converting HEU to LEU fuel is minimal since many LEU fuel fabrication facilities are in operation. In fact, the US will buy 500 MT of HEU from the NISFSU for about \$12 billion over the next 20 years. However, fuel fabrication with WGPu is

much more difficult and expensive due to the lack of such facilities and the more complicated handling procedures required with plutonium.

NAS considered the existence of surplus fissile material in its ready-for-weapons form a “clear and present danger.” NAS submitted recommendations to the US Department of Energy (DOE) which should drastically decrease the possible dangers. The recommendations stressed the importance of cooperative work between the US and the NISFSU to:

1. Ensure that neither region is producing any fissile material,
2. Exchange detailed information of each others’ WGPu stockpiles with close monitoring,
3. Prevent and protect the material from ending up in the wrong hands, and
4. Work hand in hand to devise a long-term disposition method.

NAS presented three possible options for dealing with the surplus of WGPu, and for each option outlined risks, standards and technical availability, and maturity.

1. *Indefinite Storage.* This no-action option presents several risks, which include the possibility of proliferation depending on the political stability of the possessing country. The material would be left in a weapons-usable form, which, if not well protected, could conceivably be acquired by unauthorized entities or re-used by the possessing country.

2. *Elimination.* This option is aimed at using a reactor or an accelerator to burn WGPu completely so that it has little or no remaining fissile content. This option is regarded as “overkill” since large quantities of fissile material exist in commercial spent fuel. That is, given that there are already large quantities of reactor-grade plutonium (RGPu), and that it is possible to build a small-scale nuclear weapon using RGPu, it seems illogical to go to great lengths to eliminate all WGPu.

3. *Minimized Accessibility.* This option as well as the elimination option have an added risk of handling due to the need of transportation and fabrication. This risk includes environmental hazards as well as breakdowns in security and protection from theft or diversion. Minimized accessibility is centered around making the WGPu less attractive and harder to extract for weapons' use. WGPu in this option should be as inaccessible as plutonium in spent fuel, thus the term "spent fuel standard." This can be achieved in three different approaches:

- Disposal in Deep-Boreholes. Sufficient research has been done to develop the technological base for this option, which was mainly aimed at spent fuel and high-level waste (HLW). WGPu will be protected from theft since it will be placed in very deep holes, and its recoverability by the possessing country then becomes as difficult as that from spent fuel.
- Vitrification. A strong radiation barrier is created by mixing WGPu with HLW, which makes it both inaccessible and impractical for weapons. The highly radioactive material can be vitrified and forged into glass logs, which could be placed in permanent geologic repositories.
- Mixed Oxide Fuel (MOX) in Reactors. By using WGPu as fuel in reactors, its neutronic and thermal properties are altered to resemble that of spent fuel. WGPu can be mixed with depleted uranium, whose isotopics are given in Table I, to create MOX fuel, which can be used in several different types of reactors. These reactors include US existing LWRs, NISFSU LWRs, Canadian deuterium-uranium (CANDU) reactors, several European and Japanese LWRs that already consume MOX fuel made from RGPu, and new reactors specially designed to consume MOX fuel made from WGPu. Using CANDU, European or Japanese reactors has an added risk of transporting the material across international borders. Due to the tremendous costs and time needed to license and build an advanced reactor, NAS

recommended that new reactors should be considered only if existing reactors fail to prove their technical or licensing ability to consume MOX made from WGPu. If chosen, the existing-reactor option is projected to start the mission within 10 years and complete it within 20 to 40 years, depending on the type and quantity of reactors chosen for the mission. The technical capability to burn MOX fuel has been demonstrated by several reactors in Europe and Japan that use MOX fuel made from RGPu. Although RGPu has different isotopic content than WGPu, (see Table II), NAS expects no major roadblocks in replacing RGPu with WGPu. However, the design work and calculations must be performed to confirm the speculations and to show the rate at which WGPu can be dispositioned. There is no apparent technical difficulty in fabricating MOX fuel from WGPu to be used in existing US LWRs, provided all gallium is removed from WGPu prior to fabrication. Candidate reactors include Westinghouse's and ABB-Combustion Engineering's pressurized-water reactors (PWRs) and General Electric's boiling-water reactors (BWRs). The NISFSU's respective LWR, the VVER-1000, is expected to have approximately the same handling capabilities of MOX fuel.

In its final recommendation, NAS urged the US DOE to simultaneously pursue the two more attractive options, which are the existing reactor option and the vitrification option. NAS also indicated that more technical studies need to be performed to verify the technical competence of each option. It pointed out two areas in which more research is necessary: licensing and public acceptance for the reactor option, and criticality analyses for the vitrification option.²

TABLE I
Depleted Uranium Isotopics³

Isotope	Depleted Uranium (w/o)
U-234	0.002
U-235	0.200
U-236	0.001
U-238	99.797

TABLE II
Weapons-Grade and Reactor-Grade Plutonium Isotopics³

Isotope	WGPu (w/o)	RGPu (w/o)
Pu-238	0.0	0.1
Pu-239	93.6	59.0
Pu-240	5.9	23.0
Pu-241	0.4	13.0
Pu-242	0.1	4.9

The existing LWR option seems to be the most time- and cost- effective route. Westinghouse’s PWR is one of the three main LWR types considered, each of which is capable of converting the given amount of WGPu to the “spent fuel standard” within the set time frame of 25 years.³ The objective of this research is to design fuel cycles for Vogtle Plant Unit 1, which is a four-loop Westinghouse type PWR, that will transition the plant from a full LEU to a partial-MOX-fueled reactor. Part of this research is to optimize the within-assembly WGPu enrichment distribution in MOX assemblies in order to minimize peaking.

Westinghouse submitted a report³ to DOE on June 1, 1994 in which two loading patterns of equilibrium cycles were considered for a partial-MOX four-loop plant, with integral burnable absorbers in MOX pins. A four-loop plant was chosen due to its larger capacity and longer projected operation lifetime. Vogtle Plant Unit 1 was considered as a computational prototype for this study. In that report, only equilibrium cycles were considered, with no discussion of how to transition to them. At the time of the study, DOE had no limitation on the use of integral fuel burnable absorbers (IFBA) in MOX pins. In the proposed equilibrium-cycle designs a few parameters were unacceptable and some regulatory limits, such as shutdown margins, were violated. Other parameters left some room for improvement, namely radial pin-peaking in MOX assemblies. Peaking in these designs was kept under the limits by using IFBA.

In 1996, DOE asked Westinghouse and other reactor vendors to perform further studies on using their respective reactors to burn MOX fuel from WGPu. In these studies the vendors were instructed to examine the transition from existing LEU cores to partial-MOX equilibrium cores. The vendors were further instructed to avoid using integral burnable absorbers in MOX fuel pins, because DOE did not want to rely on technology that had not been previously tested and utilized. (At present there is no fuel fabrication facility for MOX fuel with integral burnable absorber, and there is no experience using such fuel in reactors.) Additionally, DOE asked that the vendors minimize the effect of their designs on utilities, which meant for example that cycle length should not change. Therefore, one of the tasks facing Westinghouse was the design of transition cycle cores that met safety and cycle-length constraints without using IFBA in MOX pins. The work reported in this thesis was part of that task.

CHAPTER II

ANALYSIS TOOLS AND DESIGN METHODOLOGY

This chapter describes the computational analysis tools as well as the methods that we followed during the design process. Included are detailed descriptions of the computer codes that we utilized and wrote, along with relevant theory and reasoning. The step-by-step design process is also outlined in this chapter.

DESIGN PROCESS

The study upon which this thesis is based was divided into the following tasks:

- Task 1. Design of preliminary partial-MOX loading pattern, from which bounding colorsets were chosen. [Ankney, Adams, Alsaed]
- Task 2. Analysis of selected colorsets and development of preliminary within-assembly distributions for MOX assemblies using CASMO-3 [Ref. 4] and personal codes. [Alsaed]
- Task 3. Final designs of within-assembly distributions using PHOENIX-P⁵. (Required some iteration with task 4.) [Alsaed]
- Task 4. First transition cycle design using PHOENIX-P and ANC⁶. [Alsaed with considerable guidance from Ankney]
- Task 5. Second transition cycle design using PHOENIX-P and ANC. [Alsaed with guidance from Ankney]
- Task 6. Third transition cycle design using PHOENIX-P and ANC. [Alsaed]

ANALYSIS TOOLS

We utilized several well-known reactor-analysis computer codes to meet the demands of this computationally-intensive study. CASMO-3 is a 70- or 40-group assembly-wise two-dimensional (with a buckling correction for the third dimension) transport code developed by the Swedish company Studsvik. It is capable of modeling single assemblies with reflecting boundaries or colorsets with reflecting or periodic boundaries. Colorsets are four neighboring assemblies sharing one corner, as shown in Figure 1. CASMO-3 can be instructed to deplete single assemblies or colorsets and write restart files at selected burnup steps. The restart files can be read into continued depletion models. PHOENIX-P is a 42-group computer code, developed by Westinghouse, which has computational and modeling capabilities similar to CASMO-3. ANC is a Westinghouse three-dimensional two-group nodal diffusion code used for the design and analysis of full-core loading patterns and cycles.

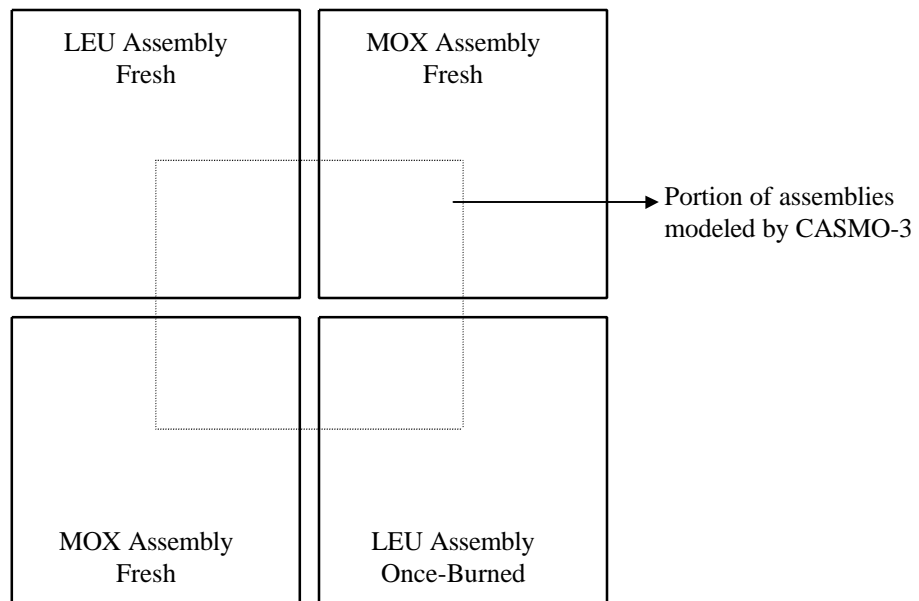


Figure 1: Schematic of a Colorset.

DESIGN METHODOLOGY

The ultimate goal of this study is to design loading patterns for a partial-MOX core that would behave much like a LEU core. In order to simplify and organize the study, we split the design process into several tasks which were performed at Texas A&M and Westinghouse. At Texas A&M, we utilized CASMO-3 to develop an understanding of the behavior of fresh MOX assemblies adjacent to fresh or burned uranium-oxide assemblies. At Westinghouse, we finalized MOX assembly enrichment distributions and designed and analyzed transition cycles.

Tasks 1 and 2

We developed a preliminary design of a loading pattern for a partial-MOX core based on LEU patterns and engineering judgment. From this pattern we chose four representative colorsets of fresh MOX and fresh and burned LEU assemblies to analyze. We used CASMO-3 to model and analyze the colorsets. We used a typical LEU-core boron letdown for all the depletions to approximate actual neutronic and spectral properties. CASMO-3 homogenizes pins into three radial regions. We specified fuel for the interior region, IFBA ring for the middle region, and air gap and cladding for the outer region for the LEU pins with IFBA. We ran CASMO-3 in two steps. First, we depleted separate MOX and LEU assemblies to the average depletion of a typical LEU reactor cycle. We chose the appropriate cards to get CAMSO-3 to write restart files at every depletion step. Second, we set up input decks for all the colorsets for which CASMO-3 read the desired assembly depletions from the previous runs, then depleted the colorsets for a full cycle. These runs presented us with parameters for these colorsets as if they were in an infinite sea of their own, since we instructed CASMO-3 to impose reflecting boundaries around the colorsets. At the time we were concerned only with radial pin-peaking to gain an

understanding of how LEU and MOX pins share power. We used this information to change and optimize the within-assembly enrichment distribution, as well as maximize the overall enrichment in MOX assemblies.

In order to gain knowledge of how these assemblies would behave in a real core, we wrote a simple program that imposes a global power shape on the optimized colorsets. Since we want the end result to look like a typical LEU core, we used assembly-average power maps at various burnup steps throughout a previous cycle for Vogtle Plant. The idea of this program is to place the assembly-average power of a typical LEU core at the center pin in each assembly, then bi-linearly interpolate between these points to generate a multiplier for each pin in the core. The multiplier represents the effect of the global power shape on pin peaking. Pin peaking is taken to be the maximum of the interpolated value or the average assembly power multiplied by the within-assembly radial peaking. Figure 2 illustrates a one-dimensional

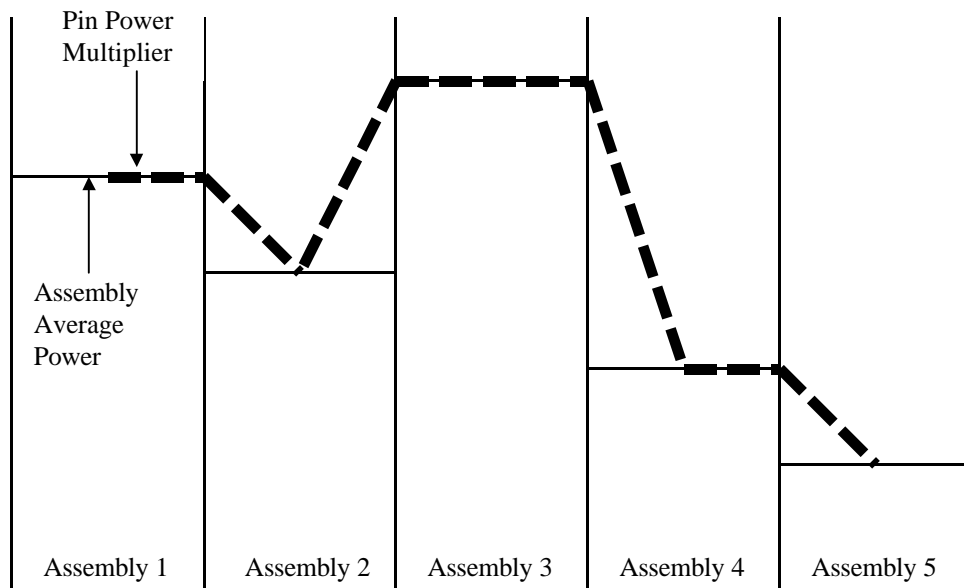


Figure 2: One-dimensional Representation of Assumed Global Power Effect

representation of this code. The first two tasks resulted in several within-assembly enrichment distributions with a variety of average overall enrichments.

Tasks 3, 4, 5, and 6

The second part of the design was performed at Westinghouse using PHOENIX-P and ANC. First, we ran PHOENIX-P for some of the colorsets designed during the first two tasks for two reasons: (1) to compare CASMO-3 pin power maps, eigenvalues and two-group cross sections to those generated by PHOENIX-P, and (2) to verify that we modeled fuel and burnable absorber pins correctly with CASMO-3. This was the end of the preliminary scoping work. We performed the following steps for the actual and final designs:

- Began designing the first transition cycle starting with the end of the current cycle for Vogtle Plant Unit 1.
- Ran PHOENIX-P to: (1) generate cross sections for the burned assemblies shuffled from the current cycle to the first transition cycle, and (2) generate cross sections for several candidate fresh LEU and MOX assemblies to be fed into the first transition cycle.
- Generated two different kinds of reflector cross sections, corner and flat, using a burned LEU assembly on the periphery and a fresh MOX assembly in the interior.
- “Punched” the cross sections for all the assemblies into a generic ANC input deck using Westinghouse’s user-friendly editing codes.
- Entered the shuffling instructions into the ANC input deck along with specific details of control rod and burnable absorber positions.

ANC depleted the loading pattern for a full cycle, generating a great deal of data including peaking information, boron levels, and power sharing in pins, nodes and assemblies, etc. The loading pattern design was an intuition-guided trial and error process until we converged upon a satisfactory design looking only at pin-peaking and cycle-length. For the cases in which pin-peaking was unacceptable, we employed an extensive iteration process. By finding out where peaks were in MOX assemblies, we corrected these flaws in new assembly designs using PHOENIX-P, then we ran ANC with the new assembly designs. After obtaining acceptable peaking and cycle-length, we performed further analyses to ensure the operability of a reactor with such a loading pattern. These analyses included the determination of moderator temperature coefficients, boron concentrations and coefficients, power coefficients, shutdown margins, and cold calculations. Once all these parameters were within the limits of the current LEU reactor cycle, we declared the cycle design a success.

CHAPTER III

WITHIN-ASSEMBLY ENRICHMENT OPTIMIZATION

This chapter describes the preliminary and final MOX assembly designs. In the preliminary designs, which were based on colorset calculations, we developed potential MOX assemblies, whose reactivity and radial pin-peaking would be acceptable when placed adjacent to LEU assemblies, limiting the burnable-absorbers to discrete types in MOX assemblies. Then, these assemblies were studied in acceptable loading pattern models. Finally, based on full-core calculations, we modified and refined the assembly designs in order to achieve acceptable peaking and reactivity characteristics.

We created a preliminary loading pattern, shown in Figure 3 for an octant-core geometry, based on engineering experience and judgment. This simple loading pattern was to be a model of the first transition cycle assuming 36 feed MOX assemblies and 45 feed LEU assemblies. We chose one kind of LEU assembly with 4.10 weight-percent (w/o) U-235 enrichment and two different enrichments of MOX assemblies. We chose the LEU assemblies to have one kind of IFBA loading--128 pins coated with 1.5 milligrams/inch of boron-10--for simplicity. We were forced to choose two kinds of MOX assemblies because some of them fall under control rod locations such as assembly (row, column) (7,3) shown in Figure 3. In order to hold down the reactivity in the MOX assemblies with the higher enrichment, we decided to put 24 wet annular burnable absorber (WABA) rods in them. Then we chose four sets of representative colorsets of MOX and LEU neighboring assemblies based on different combinations of fresh MOX and fresh and burned LEU assemblies. These colorsets in (row, column) positions were {(6,1) (6,2) (7,1) (7,2)}, {(6,2) (6,3) (7,2) (7,3)},

	1	2	3	4	5	6	7	8
1	U (R) 4.10 128 IF							
2	U 4.10 128 IF	U 4.10 128 IF						
3	U (R) 4.10 128 IF	U 4.10 128 IF	U (R) 4.10 128 IF					
4	U 4.10 128 IF	U 4.10 128 IF	U 4.10 128 IF	U 4.10 128 IF				
5	U (R) 4.10 128 IF	U 4.10 128 IF	U 4.10 128 IF	U 4.10 128 IF	U (R) 4.10 128 IF			
6	U 4.10 128 IF	U (R) 4.10 128 IF	U 4.10 128	U (R) 4.10 0	M High 24 W	M High 24 W		
7	U (R) 4.10 128 IF	M High 24 W	M (R) Low 0	M High 24 W	U (R) 4.10 128 IF	U 4.10 128 IF		
8	U 4.10 128 IF	U 4.10 128 IF	U 4.10 128 IF	U 4.10 128 IF				

- Fresh
- Once Burned
- Twice Burned

LEU/MOX (Control Rod Location)
Enrichment (w/o Fissile)
Previous Location (Row, Column)
IFBA/WABA

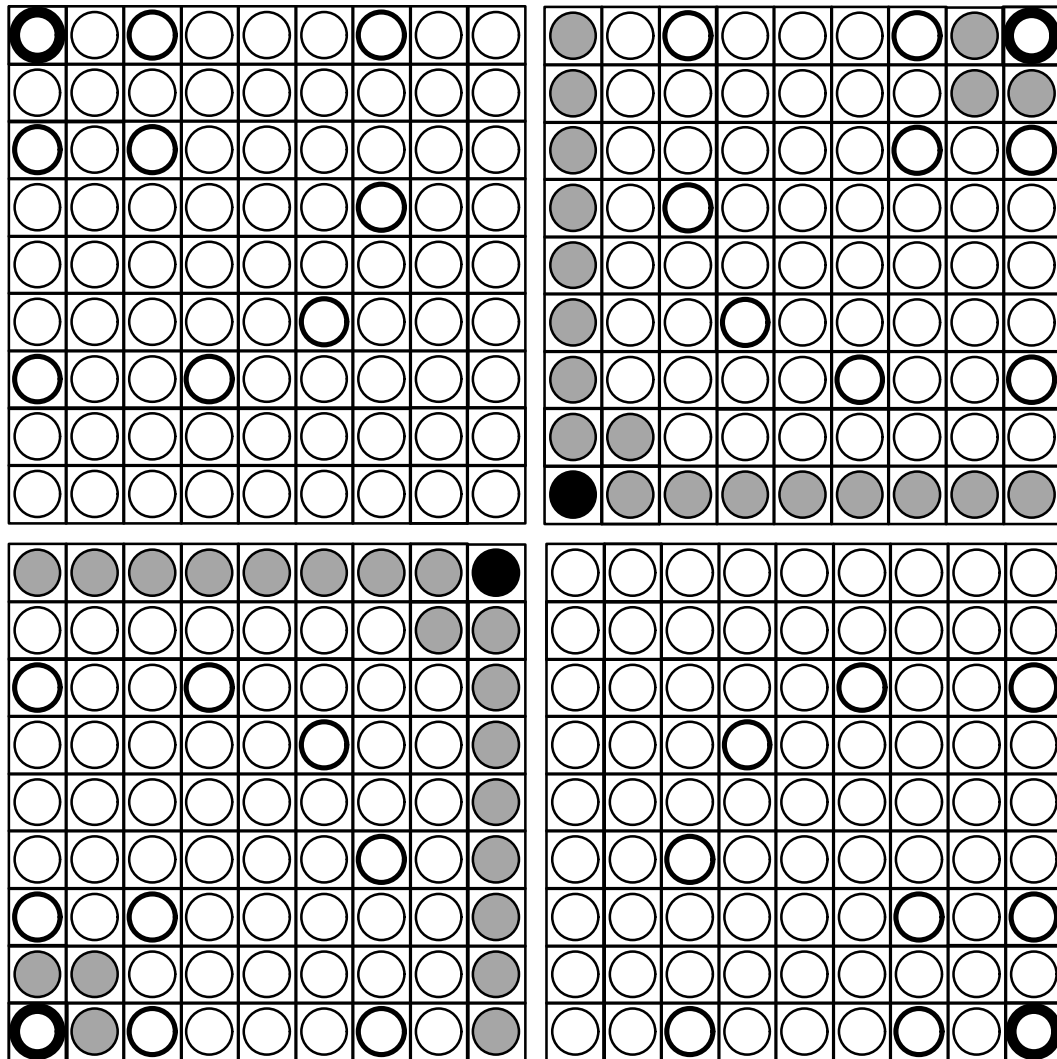
Figure 3: Engineering Judgment-Based Preliminary Design of First Transition Cycle

{{(6,4) (6,5) (7,4) (7,5)} and {(5,5) (5,6) (6,5) (6,6)}. We modeled these colorsets, as described in the previous chapter, using CASMO-3 along with its 70-group cross sections library. In modeling these colorsets, the only variable was MOX assembly designs, since we decided on one LEU and IFBA assembly type. In designing MOX assemblies, we had to iterate on two things: (1) average WGPu enrichment and (2) enrichment distribution. The approach we took towards the average WGPu enrichment in MOX assemblies was to maximize it within reason. In other words, we had only one limit: radial pin-peaking. The worst peaking seemed to be in the corner pins of MOX assemblies adjacent to LEU assemblies. Peaking became more easily controlled in the assemblies with the higher WGPu enrichment by decreasing the enrichments in the corner pins and those around the periphery adjacent to uranium-oxide pins, and by raising the enrichment of interior MOX pins. We decided that three different enrichments was a reasonable number to be used within a MOX assembly, for practical manufacturing reasons. The MOX assembly with the lower enrichment, namely position (7,3), had two peaking problems: (1) around the periphery adjacent to LEU assemblies, and (2) around the water-filled guide and instrumentation thimbles. We found that no distribution would correct the peaking problem with reasonable WGPu enrichment (above 4.0 w/o fissile). Consequently, we designed these assemblies to have a relatively low enrichment (3.0 w/o fissile) without any kind of enrichment distribution.

CASMO-3 generates relative pin powers at various burnup steps, roughly every 1,000 MWD/MTM, throughout the specified cycle length of 17,500 MWD/MTM. CASMO-3 calculates these relative pin powers assuming an infinite geometry of colorsets, which is far from the realistic finite and leaky core geometry. We wrote a code, described in the previous chapter, to impose a global-core power shape on those colorsets assuming their positions in the preliminary core design. For

this code, we used assembly average power maps from cycle 7 of the Vogtle plant Unit 1. We used these maps at burnup steps of 0, 150, 9,000 and 20,000 MWD/MTM. In order to generate the correct multipliers at the correct burnup steps in the CASMO-3 runs, the code linearly interpolated on these assembly average power maps. In doing so, we hoped that the placement of MOX assemblies in the core would have insignificant change on the global-core power shape. The current radial pin-peaking limit for the Vogtle Plant Unit 1 is 1.528. We tried to stay conservatively under this limit. Since we had only one limit of pin-peaking and a wide range of average MOX assembly enrichments and distributions, we designed several MOX assemblies that would meet the peaking limit with the simulated global-core power shape imposed. A zoned example for the $\{(6,4) (6,5) (7,4) (7,5)\}$ colorset is shown in Figure 4 in quarter-assembly geometry. Figure 5 illustrates the decrease in radial pin-peaking in that colorset when well-zoned MOX assemblies replace flat ones with comparable average enrichments. Figure 6 shows the effect of the simulated global-core power shape on radial pin-peaking compared to that generated by CASMO-3 in infinite geometry.

During the first transition cycle design, we avoided feeding in MOX assemblies without WABA rods since their average enrichment would have to be relatively low. We knew this would not add enough reactivity for an 18-month cycle. We also avoided placing MOX assemblies towards the interior part of the core for reasons to be discussed in the next chapter. This left us with 28 possible positions for zoned MOX assemblies, as shown in Figure 7, for the final design of the first



- 3.0128 w/o Pu-fissile
- 3.5150 w/o Pu-fissile
- 5.0214 w/o Pu-fissile (in MOX assembly)
- GUIDE THIMBLE
- INSTRUMENTATION THIMBLE
- 4.1 w/o U-235 (in UO₂ assembly)

Figure 4: Quadrants of a MOX-LEU Colorset

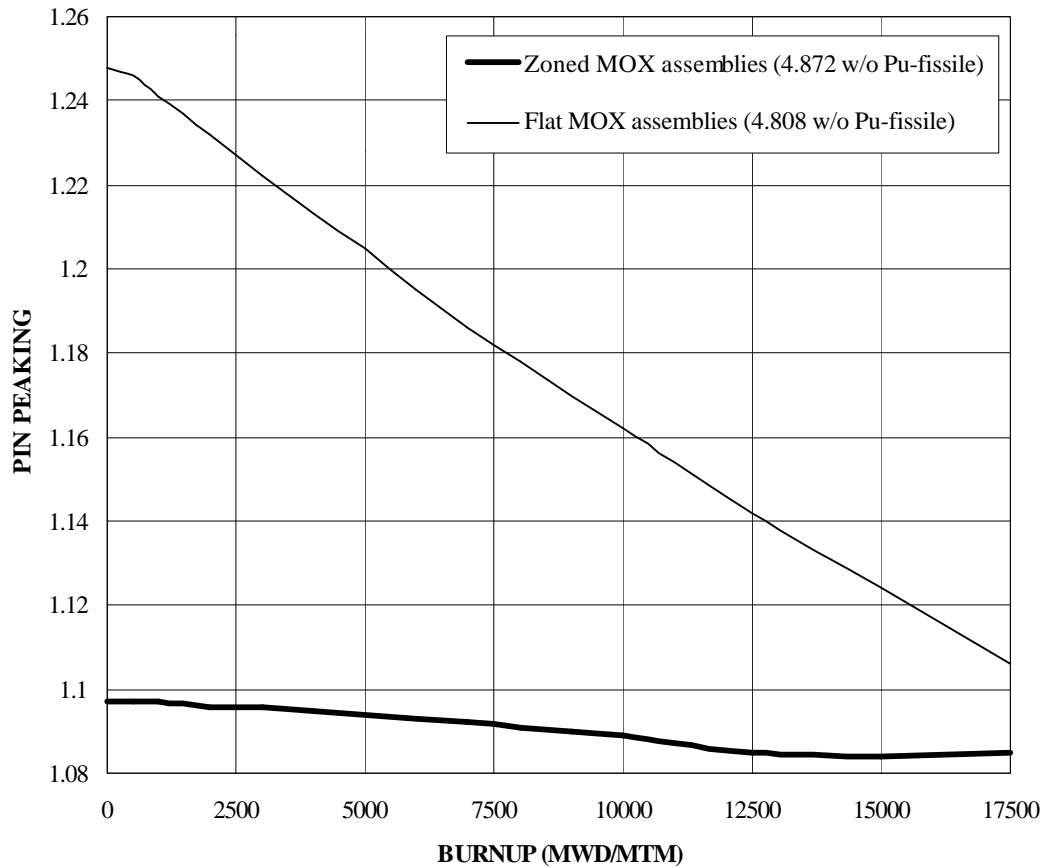


Figure 5: Pin-peaking as a Function of Burnup in a MOX-LEU Colorset with Zoned and Flat MOX Assemblies

transition cycle. We discovered that two kinds of MOX assemblies were still required: (1) one with relatively high enrichment and, (2) the other with relatively low enrichment. This allowed us to avoid localizing the power around the MOX assemblies and at the same time have enough reactivity for a full cycle. The preliminary MOX assembly designs, which are based on CASMO-3 colorset

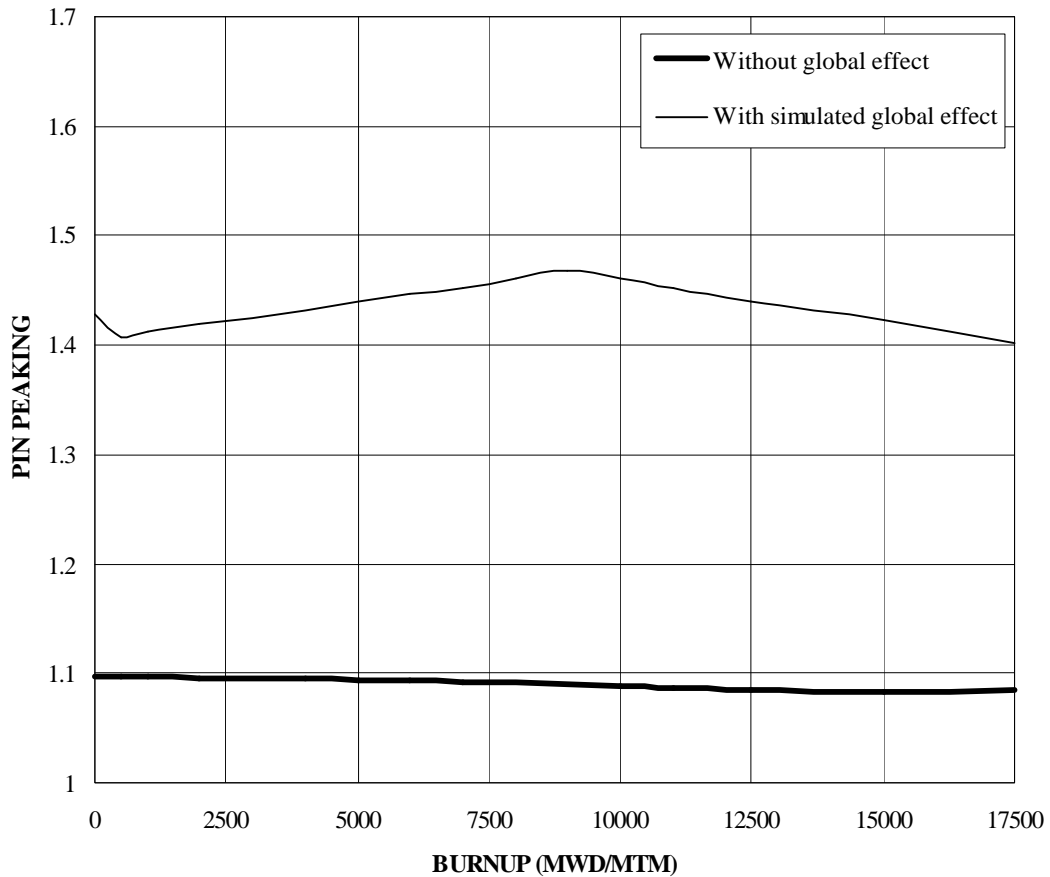


Figure 6: Effect of Simulated Global Power Shape on Pin-peaking.

modeling and the simple interpolation program (described previously) for the global power shape, were put through a stringent test in the actual first transition cycle design. ANC conveniently reconstructs pin powers when the appropriate input cards are selected. By thoroughly studying the pin power maps in the MOX assemblies, the true iteration process of MOX assembly designs starts. We found that there was still some high peaking in the periphery pins of MOX assemblies adjacent to fresh

	1	2	3	4	5	6	7	8
1	U (R) 4.2 128 IF							
2	U 4.20 24 W	U 4.20 16 IF						
3	U (R) 4.50 104 IF	U 4.20 24 W	U (R) 4.50 104 IF					
4	U 4.50 24 W	U 4.50 104 IF	U 4.50 64 IF	U 4.50 64 IF				
5	U (R) 4.50 104 IF	U 4.50 24 W	U 4.50 104 IF	U 4.50 24 W	U (R) 4.50 104 IF			
6	U 4.20 24 W	U (R) 4.20 104 IF	U 4.20 24 W	U (R) 4.20 104 IF	M 3.992 24 W	M 3.992 24 W		
7	U (R) 4.20 80 IF	M 4.515 24 W	U (R) 4.5 104 IF	M 4.515 24 W	U (R) 4.50 104 IF	U 4.20 16 IF		
8	U 4.50 104 IF	U 4.50 48 IF	U 4.20 64 IF	U 4.50 128 IF				

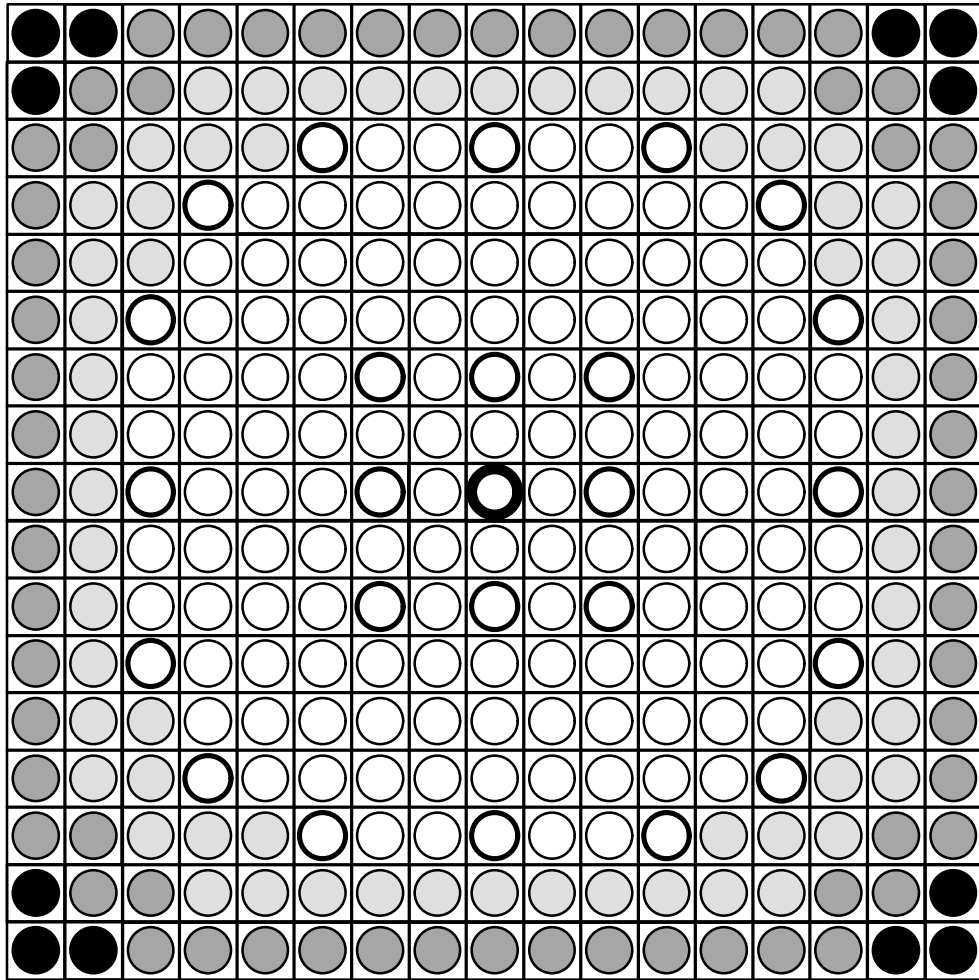
- Fresh
- Once Burned
- Twice Burned

LEU/MOX (Control Rod Location)
Enrichment (w/o Fissile)
Previous Location (Row, Column)
IFBA/WABA

Figure 7: Final Design of the First Transition Cycle

and burned LEU assemblies, while at the same time, there was low power sharing in the interior pins of MOX assemblies, especially around the WABA rods and the central instrumentation guide thimble. The corner pins seemed to be most sensitive since they are surrounded with more water and are exposed to a softer spectrum from neighboring LEU pins. The corner pins one row in from the periphery were exposed to a similar spectrum but with somewhat weaker intensity. After several iterations, we converged on two assembly designs that met peaking limits as well as added enough reactivity to the core to last a full 18-month cycle with an average burnup of 21,564 MWD/MTM. These two MOX assembly designs are shown in Figures 8 and 9 for the high and low average enrichments, respectively. Figure 10, a plot of core pin-peaking when the two final MOX assembly designs are used, clearly shows that peaking throughout the cycle stays well below the limit of 1.528. When flat MOX assemblies with comparable enrichments are used in place of the zoned MOX assemblies, peaking highly exceeds the limit almost throughout the entire cycle.

The final test for these assembly designs is in the second and third transition cycles, when these assemblies are once- or twice-burned, especially if they are placed in high power locations. We found that these MOX assemblies do not exceed the peaking limit even after the WABA rods were pulled out. We will show this in the Chapter IV, "Transition Cycles Design and Analyses," for the second and third transition cycle designs.









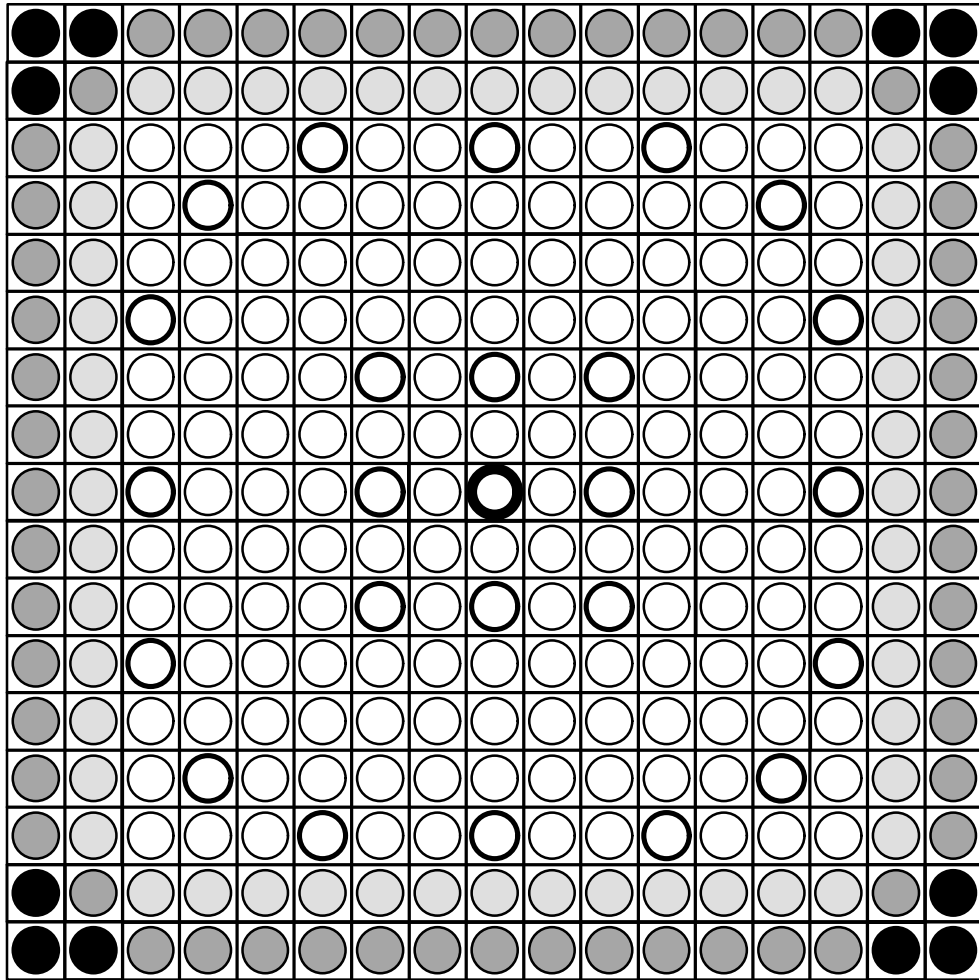
-  2.50 w/o Pu-fissile
-  3.00 w/o Pu-fissile
-  4.50 w/o Pu-fissile
-  5.50 w/o Pu-fissile
-  GUIDE THIMBLE
-  INSTRUMENTATION THIMBLE

Figure 8: MOX Assembly with 4.515 w/o Pu-fissile Average Enrichment




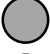
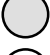



-  2.50 w/o Pu-fissile
-  3.00 w/o Pu-fissile
-  4.00 w/o Pu-fissile
-  4.50 w/o Pu-fissile
-  GUIDE THIMBLE
-  INSTRUMENTATION THIMBLE

Figure 9: MOX Assembly with 3.992 w/o Pu-fissile Average Enrichment

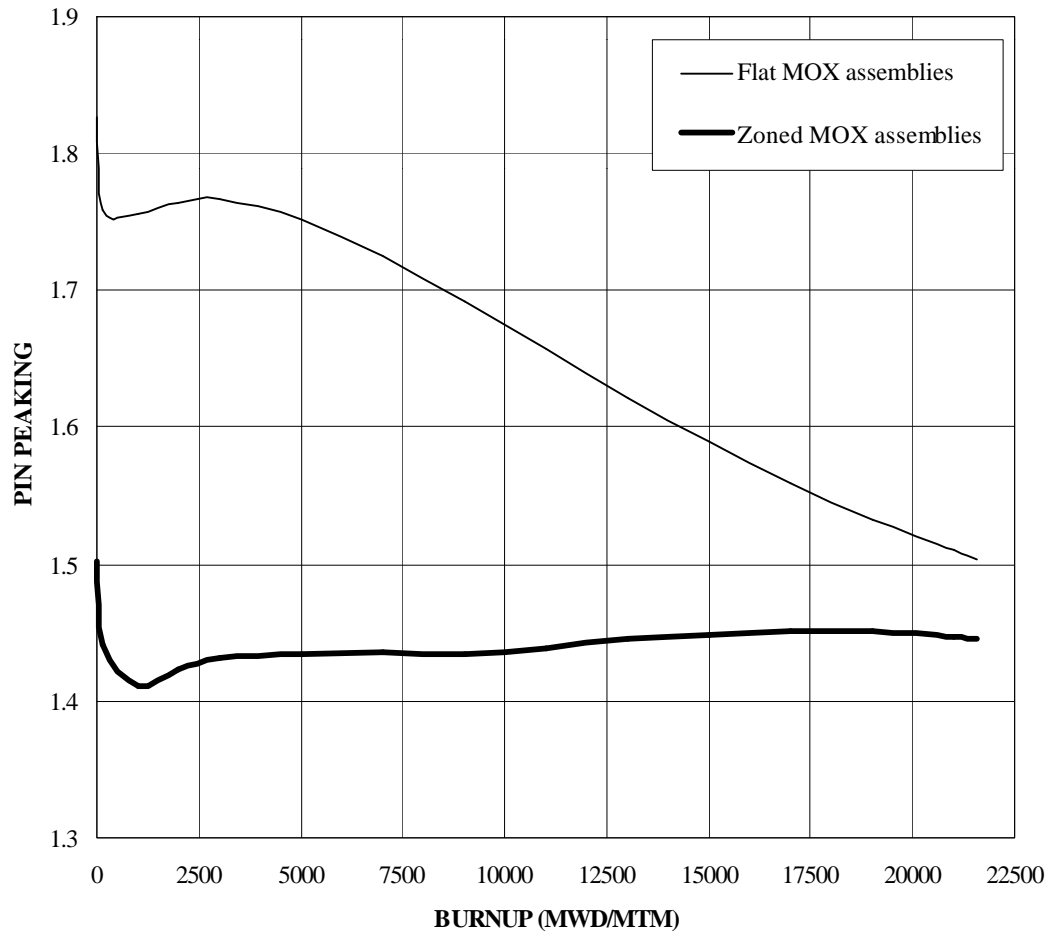


Figure 10: Effect of Zoned MOX Assemblies on Pin-peaking in a Partial MOX Core

CHAPTER IV

TRANSITION CYCLES DESIGN AND ANALYSIS

Ultimately, this study will help in moving toward an equilibrium stage in which the model reactor, Vogtle, will operate safely and much like a typical LEU fueled reactor with a reasonable MOX fuel loading. In order to reach that partial-MOX equilibrium stage, we must achieve a successful transition from an all-LEU reactor. Since the end result will be a partial-MOX core, the reloads will also be partial-MOX. Assuming that the equilibrium core will be approximately one-third MOX, the reloads are chosen to be approximately one-third MOX. This means at least three transition cycles are required in order to reach some type of an equilibrium phase. It is important to remember that throughout each transition cycle, the reactor should comply with all the operating limits and parameters of an all-LEU core, some of which are listed in Table III.

FIRST TRANSITION CYCLE

Maximizing the WGPu loading is desirable in order to achieve DOE's fast-disposition objective; however, this must be done within the constraints of operational safety and comparable operability to an LEU core. We chose a typical reload of 92 feed assemblies, which consisted of 28 MOX assemblies and 64 LEU assemblies. In order to meet plant regulations of minimized vessel irradiation, we designed a low-leakage loading pattern with once- and twice-burned assemblies around

TABLE III
Vogtle Specific Operating and Design Parameters³

Parameter	Value
Number of fuel assemblies	193
Number of control rods, rodlets per cluster	53, 24
Control rod material	Ag-In-Cd (80/15/5)
Power level ($M_{w_{th}}$), electrical output (MW_e)	3565, 1232
System pressure (psia)	2250
Hot zero power (HZP) moderator temperature ($^{\circ}F$)	557.0
Hot full power (HFP) moderator temperature ($^{\circ}F$)	589.6
Cold zero power (CZP) moderator temperature ($^{\circ}F$)	68
CZP system pressure (psia)	14.7
Fuel lattice, fuel rods per assembly	17 x 17, 264
Fuel pellet OD, Fuel rod OD (in.)	3.088, 0.360
Cladding material	Zircaloy-4
Active fuel length (in.)	144
Design radial pin-peaking ($F_{\Delta H}$)	1.528
Design point-wise peaking (F_Q)	2.50
Moderator temperature coefficient (MTC) limit (pcm/ $^{\circ}F$)	+7 up to 70% power, +0 at 100% power
Core loading in metric ton metal (MTM)	81.6
Target cycle length (megawatt days (MWD)/MTM)	21,564
(Months)	18
Capacity factor (%)	90
Target effective full power days	493
Target discharge burnup (MWD/MTM)	40,000 to 50,000
Maximum pin burnup (MWD/MTM)	62,000
Shutdown margin (SDM) ($\% \Delta \rho$)	1.3

the periphery. Locations of MOX assemblies were also limited to non-control rod positions since each MOX feed assembly contained 24 WABA rods, in compliance with DOE prohibition against using integral burnable absorbers in MOX fuel. The relatively high number of WABA rods is needed to suppress the reactivity in the highly reactive MOX assemblies relative to LEU assemblies. The large difference in

reactivity is due to Pu-239's much higher thermal and resonance-integral fission cross sections, relative to those of U-235, as presented in Table IV.

TABLE IV
Thermal and Resonance-Integral Cross Sections for U-235 and Pu-239⁷

Cross section (barn)	U-235	Pu-239
Capture, σ_c	98.4	270.2
Fission, σ_f	583.9	741.7
Absorption, σ_a	682.3	1011.9
Resonance integral, capture	139.2	193.9
Resonance integral, fission	281.7	303.5

These cross sections clearly indicate that Pu-239 is a much stronger absorber than U-235, implying that the WABA rods are worth less in MOX assemblies than they are in LEU assemblies. The domination of Pu-239 over U-235 will cause some power shift and localize it in and around MOX assemblies. Due to leakage around the periphery, interior assemblies carry a larger fraction of the overall power load. Placing MOX assemblies in interior locations dramatically steepens the power shape and concentrates more of it towards the interior where the higher reactive MOX assemblies reside. The above regulations and physics laws limit the first 28 feed MOX assemblies to be placed one row in from the periphery, which typically are low-power locations, in the hope that the power shift to these locations will help flatten the power shape. With 92 feed assemblies, there were 101 once- and twice-burned assemblies. We chose the least-burned assemblies from the previous cycle to make up the 101 burned assemblies: all 84 once-burned and 17 twice-burned assemblies. When shuffling these assemblies into the current loading pattern, we

carefully maintained octant symmetry. The loading pattern design was a lengthy process of trial and error guided by engineering judgment and involving numerous ANC runs for the global core analysis and PHOENIX-P runs for generation of cross-sections for feed assemblies. We aimed the iteration process at getting acceptable peaking as well as the desired cycle length. We controlled cycle length by varying enrichment and burnable-absorber loading; we minimized pin-peaking by zoning the enrichment in MOX assemblies (see previous chapter). This was coupled with the optimum placement of all feed and burned assemblies in the core. Figure 11 is a step-by-step flow chart of the design process.

Our final design of the first transition cycle is shown in Figure 12. We achieved fine-tuning of the loading pattern by rotating the burned assemblies to locally optimize peaking as well as burnup by exposing the more reactive sides of each assembly to the higher burnup locations. This evens out the burnup in all the pins in each assembly.

Figures 13, 14, and 15 present layouts of power, burnup and pin-peaking distribution in the proposed loading pattern design at beginning of cycle (BOC), middle of cycle (MOC), and end of cycle (EOC). These three figures clearly indicate a somewhat flattened radial power shape with the MOX assemblies sharing more of the power than LEU assemblies would in the same positions. Due to the harder spectrum in MOX assemblies, B-10 in WABA rods in MOX burns out at a slower rate than it would in WABA rods in LEU assemblies. This causes power shifts from MOX assemblies to LEU assemblies midway through the cycle. Late in the cycle, when significant burnout of B-10 is achieved, the power shifts back to MOX

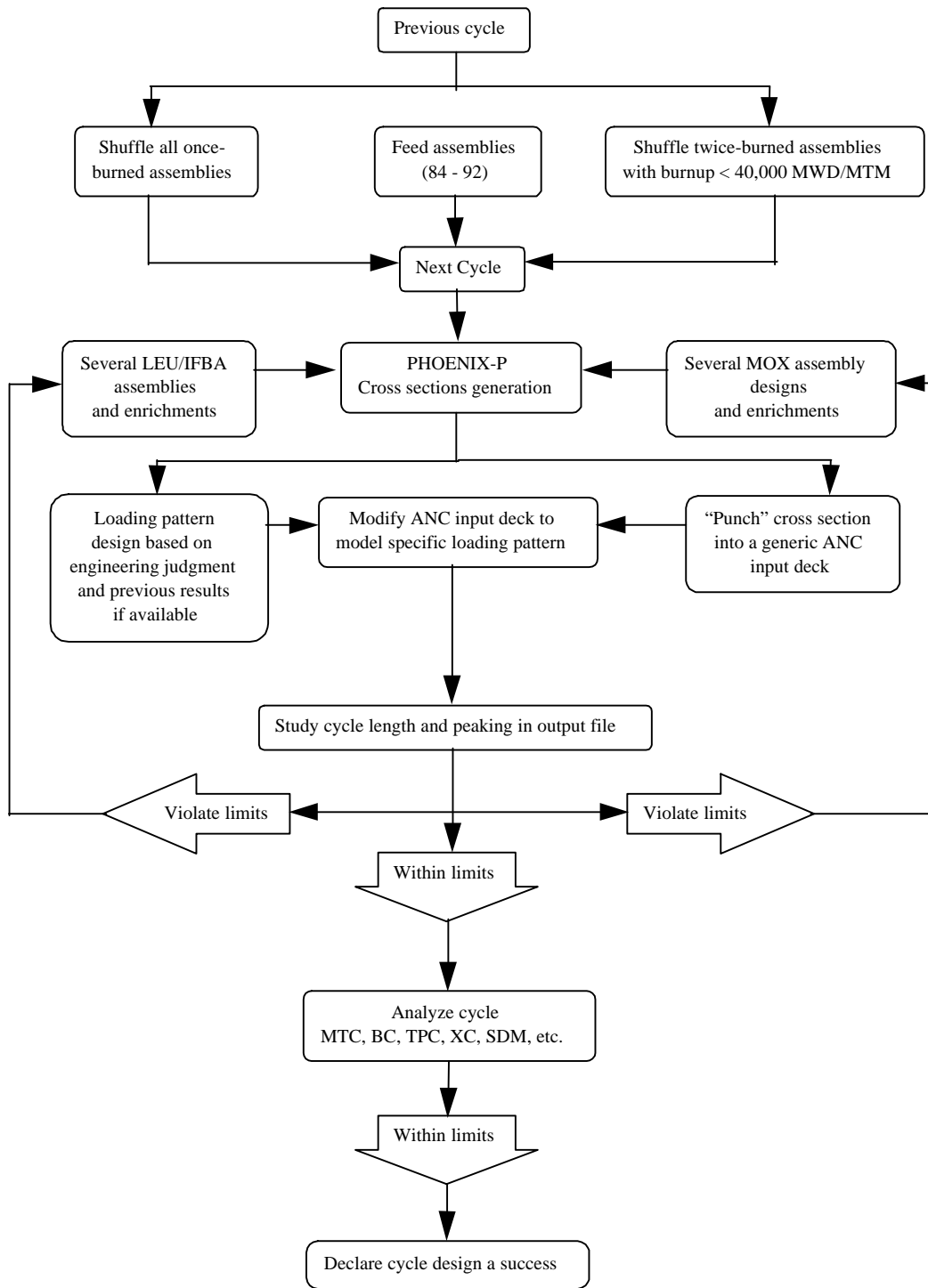


Figure 11: Step-by-Step Design of a Transition Cycle

	1	2	3	4	5	6	7	8
1	U (R) 4.2 128 IF							
2	U 4.20 24 W	U 4.20 16 IF						
3	U (R) 4.50 104 IF	U 4.20 24 W	U (R) 4.50 104 IF					
4	U 4.50 24 W	U 4.50 104 IF	U 4.50 64 IF	U 4.50 64 IF				
5	U (R) 4.50 104 IF	U 4.50 24 W	U 4.50 104 IF	U 4.50 24 W	U (R) 4.50 104 IF			
6	U 4.20 24 W	U (R) 4.20 104 IF	U 4.20 24 W	U (R) 4.20 104 IF	M 3.992 24 W	M 3.992 24 W		
7	U (R) 4.20 80 IF	M 4.515 24 W	U (R) 4.5 104 IF	M 4.515 24 W	U (R) 4.50 104 IF	U 4.20 16 IF		
8	U 4.50 104 IF	U 4.50 48 IF	U 4.20 64 IF	U 4.50 128 IF				

- Fresh
- Once Burned
- Twice Burned

LEU/MOX (Control Rod Location)
Enrichment (w/o Fissile)
Previous Location (Row, Column)
IFBA/WABA

Figure 12: Final Design of the First Transition Cycle

assemblies. For example, the LEU assembly (2,1) in Figure 13 at BOC is running at an assembly average power of 1.168 while the MOX assembly (6,5) in the same figure is running at an assembly average power of 1.249. At MOC in Figure 14, the assembly average power in the LEU assembly (2,1) increases to 1.341 due the relatively fast burnout of B-10 in the WABA rods, while the assembly average power in the MOX assembly (6,5) decreases to 1.098 since the B-10 in the WABA rods burns out at a slower rate. At EOC in Figure 15, the assembly average power in the LEU assembly (2,1) decreases to 1.254, while the power in the MOX assembly (6,5) increases slightly to 1.183, flattening out the power shape due to higher burnup in higher power locations. This power shift was more pronounced in earlier designs of the first transition cycle when we attempted to use IFBA in all the LEU feed assemblies. Since B-10 is denser and “layered” in WABA rods, it burns out at a slower rate than B-10 in IFBA coating, which is relatively less dense and “thinner” so that more B-10 nuclei are exposed to neutrons.

	1	2	3	4	5	6	7	8
1	U (R) 0.930 0.984 38798							
2	U 1.168 1.316 172	U 1.206 1.323 20263						
3	U (R) 1.160 1.193 28656	U 1.213 1.340 179	U (R) 1.174 1.223 26023					
4	U 1.262 1.378 187	U 1.165 1.218 27581	U 1.155 1.227 26329	U 1.185 1.243 26308				
5	U (R) 1.174 1.211 28217	U 1.249 1.376 187	U 1.154 1.199 28548	U 1.243 1.274 192	U (R) 1.197 1.299 26089			
6	U 1.196 1.308 180	U (R) 1.129 1.185 28686	U 1.225 1.362 185	U (R) 1.105 1.200 28121	M 1.249 1.441 192	M 0.982 1.304 152		
7	U (R) 1.087 1.295 164	M 1.155 1.406 175	U (R) 1.047 1.288 159	M 1.021 1.340 156	U (R) 0.739 1.059 113	U 0.415 0.810 21978		
8	U 0.463 0.748 28246	U 0.367 0.605 47189	U 0.440 0.741 24134	U 0.286 0.611 42143				

Assembly Type (CR Location)
Assembly Average Power
Assembly $F_{\Delta H}$
Assembly Average Burnup

Figure 13: Layout of Assembly Average Power, Radial Pin-peaking, and Assembly Average Burnup at BOC (150 MWD/MTM). (Assembly with hottest pin is shaded.)

	1	2	3	4	5	6	7	8
1	U (R) 0.971 1.003 49102							
2	U 1.341 1.392 13950	U 1.177 1.254 33226						
3	U (R) 1.131 1.173 41127	U 1.315 1.387 14019	U (R) 1.048 1.114 37976					
4	U 1.373 1.418 14643	U 1.084 1.150 39766	U 1.004 1.050 37895	U 1.019 1.072 37927				
5	U (R) 1.138 1.182 40858	U 1.349 1.412 14443	U 1.057 1.116 40469	U 1.277 1.329 13902	U (R) 1.026 1.124 37776			
6	U 1.359 1.417 14401	U (R) 1.109 1.166 40976	U 1.344 1.408 14287	U (R) 1.012 1.097 39431	M 1.098 1.270 12421	M 0.856 1.104 9649		
7	U (R) 1.206 1.420 13128	M 1.191 1.439 1.3069	U (R) 1.191 1.422 12681	M 1.007 1.300 11033	U (R) 0.775 1.069 8214	U 0.394 0.728 26217		
8	U 0.510 0.787 33690	U 0.408 0.649 51470	U 0.489 0.789 29282	U 0.310 0.642 45371				

Assembly Type (CR Location)
Assembly Average Power
Assembly $F_{\Delta H}$
Assembly Average Burnup

Figure 14: Layout of Assembly Average Power, Radial Pin-peaking, and Assembly Average Burnup at MOC (11,000 MWD/MTM). (Assembly with hottest pin is shaded.)

	1	2	3	4	5	6	7	8
1	U (R) 0.927 0.954 59037							
2	U 1.254 1.303 27690	U 1.082 1.144 45105						
3	U (R) 1.044 1.080 52566	U 1.238 1.300 27519	U (R) 1.000 1.042 48306					
4	U 1.286 1.332 28711	U 1.021 1.072 50833	U 0.980 1.032 48306	U 1.008 1.061 48604				
5	U (R) 1.059 1.099 52432	U 1.284 1.342 28392	U 1.027 1.080 51460	U 1.286 1.340 27528	U (R) 1.048 1.124 48752			
6	U 1.283 1.338 28401	U (R) 1.054 1.103 52387	U 1.317 1.377 28435	U (R) 1.027 1.096 50218	M 1.183 1.351 24508	M 0.977 1.231 19337		
7	U (R) 1.163 1.324 25638	M 1.191 1.445 25640	U (R) 1.195 1.374 25335	M 1.080 1.393 22074	U (R) 0.892 1.188 17073	U 0.479 0.823 30824		
8	U 0.555 0.804 39290	U 0.458 0.685 55993	U 0.550 0.830 34761	U 0.366 0.689 48915				

Assembly Type (CR Location)
Assembly Average Power
Assembly $F_{\Delta H}$
Assembly Average Burnup

Figure 15: Layout of Assembly Average Power, Radial Pin-peaking, and Assembly average burnup at EOC (21,564 MWD/MTM). (Assembly with hottest pin is shaded.)

SECOND TRANSITION CYCLE

Following the design procedure outlined in Figure 11, we found that we needed 84 feed assemblies for the second transition cycle. For those feed assemblies, we chose 48 LEU and 36 MOX assemblies. We fed in more MOX assemblies this time since we had burned MOX assemblies shuffled from the previous cycle in interior and periphery locations. This helped shape the radial power distribution. Since MOX holds its reactivity longer than LEU, because it is more reactive at the same burnup with the same initial reactivity, we had to place some fresh WABA rods in some internally located burned MOX assemblies. We helped flatten the power shape by placing relatively reactive burned assemblies around the periphery, which made the core somewhat leakier. The core retained its low-leakage characteristic, though, since no fresh assemblies were placed around the periphery. Because the core is leakier and had only 84 fresh assemblies, we discovered that we needed only one kind of LEU assembly, and we still attained an acceptable power distribution. This single kind of LEU assembly had to compensate for the lost reactivity of the 8 bundles, relative to the previous cycle, that were “missing.” In order to get a cycle length of 21,564 MWD/MTM, we had to raise the enrichment in the LEU assemblies to 4.9 w/o, which is still under the maximum allowable LEU enrichment licensed for Vogtle of 4.95 w/o. After going through several iterations of loading patterns and raising LEU enrichment, we achieved an optimized design for the second transition cycle as shown in Figure 16. Maps of assembly average power, radial pin peaking, and assembly average burnup are shown in Figures 17, 18 and 19 at BOC, MOC and EOC, respectively. The figures show a relatively flat radial power distribution comparable to that of LEU cores.

	1	2	3	4	5	6	7	8
1	U (R) 4.2 (3,8) 64 IF							
2	U 4.90 24 W	M 3.992 (6,6) 4 W						
3	U (R) 4.50 (3,6) 0	U 4.50 (7,5) 104 IF	U (R) 4.50 (1,4) 0					
4	U 4.90 24 W	M 4.515 (7,4) 24 W	U 4.90 24 W	U 4.20 (1,7) 80 IF				
5	U (R) 4.20 (8,3) 64 IF	U 4.90 24 W	U 4.50 (7,3) 104 IF	U 4.20 (3,2) 0	U (R) 4.90 104 IF			
6	U 4.50 (6,3) 0	U (R) 4.50 (5,4) 0	M 3.992 24 W	U (R) 4.50 (5,2) 0	M 3.992 24 W	M 4.515 24 W		
7	U (R) 4.90 64 IF	M 4.515 24 W	U (R) 4.90 104 IF	M 4.515 24 W	U (R) 4.90 48 IF	U 4.20 (7,6) 16 IF		
8	U 4.50 (8,1) 104 IF	M 3.992 (6,5) 0	M 4.515 (7,2) 0	U 4.20 (2,1) 0				

- Fresh
- Once Burned
- Twice Burned

LEU/MOX (Control Rod Location)
Enrichment (w/o Fissile)
Previous Location (Row, Column)
IFBA/WABA

Figure 16: Final Design of the Second Transition Cycle

	1	2	3	4	5	6	7	8
1	U (R) 0.978 1.013 34885							
2	U 1.218 1.331 180	M 1.228 1.357 19511						
3	U (R) 1.078 1.148 28573	U 1.157 1.242 17236	U (R) 1.065 1.127 28896					
4	U 1.111 1.225 164	M 1.026 1.161 22216	U 1.163 1.293 172	U 1.025 1.086 25789				
5	U (R) 0.883 0.960 34889	U 1.151 1.327 171	U 1.096 1.178 25491	U 1.045 1.131 27730	U (R) 1.317 1.402 199			
6	U 1.043 1.128 28568	U (R) 1.087 1.196 27628	M 1.335 1.426 202	U (R) 1.075 1.164 28572	M 1.260 1.433 193	M 1.006 1.352 154		
7	U (R) 1.222 1.384 185	M 1.226 1.450 186	U (R) 1.156 1.321 176	M 1.091 1.390 166	U (R) 0.869 1.216 133	U 0.365 0.696 30876		
8	U 0.472 0.794 39360	M 0.581 0.921 24581	M 0.588 0.975 25725	U 0.369 0.659 27764				

Assembly Type (CR Location)
Assembly Average Power
Assembly $F_{\Delta H}$
Assembly Average Burnup

Figure 17: Layout of Assembly Average Power, Radial pin-peaking, and Assembly Average Burnup at BOC (150 MWD/MTM). (Assembly with hottest pin is shaded.)

	1	2	3	4	5	6	7	8
1	U (R) 1.013 1.049 45739							
2	U 1.370 1.437 14344	M 1.193 1.421 32650						
3	U (R) 1.088 1.136 40276	U 1.156 1.247 29820	U (R) 1.077 1.134 40533					
4	U 1.339 1.416 13472	M 1.162 1.351 34076	U 1.341 1.410 13809	U 1.016 1.084 36888				
5	U (R) 0.950 1.019 44283	U 1.329 1.403 13659	U 1.068 1.144 37198	U 0.979 1.031 38669	U (R) 1.330 1.430 14851			
6	U 1.000 1.044 39633	U (R) 1.028 1.112 39160	M 1.251 1.373 14054	U (R) 0.966 1.036 39542	M 1.143 1.323 13009	M 0.915 1.240 10341		
7	U (R) 1.199 1.352 13561	M 1.156 1.380 13066	U (R) 1.203 1.399 13233	M 1.021 1.286 11505	U (R) 0.839 1.142 9355	U 0.356 0.637 34735		
8	U 0.466 0.748 44504	M 0.561 0.861 30829	M 0.581 0.948 32131	U 0.376 0.652 31808				

Assembly Type (CR Location)
Assembly Average Power
Assembly $F_{\Delta H}$
Assembly Average Burnup

Figure18: Layout of Assembly Average Power, Radial Pin-peaking, and Assembly Average Burnup at MOC (11,000 MWD/MTM). (Assembly with hottest pin is shaded.)

	1	2	3	4	5	6	7	8
1	U (R) 0.950 0.991 56119							
2	U 1.282 1.348 28472	M 1.085 1.180 44687						
3	U (R) 1.014 1.065 51509	U 1.091 1.183 41753	U (R) 1.018 1.073 51681					
4	U 1.334 1.411 27899	M 1.163 1.345 46455	U 1.329 1.408 28126	U 1.003 1.064 47547				
5	U (R) 0.954 1.021 54871	U 1.334 1.417 27903	U 1.050 1.125 48390	U 0.964 1.006 48926	U (R) 1.302 1.397 28702			
6	U 0.981 1.018 50091	U (R) 1.003 1.074 49797	M 1.245 1.369 27206	U (R) 0.962 1.022 49675	M 1.174 1.361 25179	M 0.986 1.324 20308		
7	U (R) 1.183 1.312 26062	M 1.164 1.409 25247	U (R) 1.201 1.364 25901	M 1.068 1.353 22472	U (R) 0.899 1.189 18484	U 0.413 0.693 38751		
8	U 0.505 0.772 49579	M 0.587 0.870 36818	M 0.610 0.966 38368	U 0.421 0.693 35998				

Assembly Type (CR Location)
Assembly Average Power
Assembly $F_{\Delta H}$
Assembly Average Burnup

Figure 19: Layout of Assembly Average Power, Radial Pin-peaking, and Assembly Average Burnup at EOC (21,564 MWD/MTM). (Assembly with hottest pin is shaded.)

THIRD TRANSITION CYCLE

The third transition cycle design followed a relatively simple path from the second transition cycle design, as we chose the same number of feed assemblies (84) with the same LEU to MOX ratio (48 LEU and 36 MOX). We placed the feed assemblies in the same locations as in the second transition cycle. We used WABA rods in some internally-located once-burned MOX assemblies. We placed once- and twice-burned MOX assemblies mainly around the periphery. In order to flatten out the power near the center of the core and extract as much energy as possible from all the assemblies, we shuffled a relatively reactive thrice-burned assembly into the central position of this cycle. The once-burned LEU assemblies in this cycle, shuffled in from the previous cycle, had an initial reactivity of 4.9 w/o, which left them a significant amount of reactivity to offer. As a result of that, the LEU feed assemblies into this cycle had an enrichment of only 4.5 w/o, which was enough for a 21,564 MWD/MTM cycle. After a few loading-pattern and LEU-enrichment iterations, we converged on an optimized and acceptable loading pattern shown in Figure 20. The distributions of assembly average power, radial pin peaking and assembly average burnup are given in Figures 21, 22 and 23 at BOC, MOC and EOC, respectively. The loading pattern and power and burnup distributions in this cycle are not very different from those of the second transition cycle. The difference will even be more subtle in a fourth transition cycle which would have the same number and ratio of feed assemblies. This makes it safe to say that the third transition cycle resembles an equilibrium partial-MOX cycle.

	1	2	3	4	5	6	7	8
1	U (R) 4.2 (7,6) 16 IF							
2	U 4.50 24 W	M 4.515 (6,6) 4 W						
3	U (R) 4.90 (2,1) 0	U 4.90 (7,5) 48 IF	U (R) 4.90 (5,5) 104 IF					
4	U 4.50 24 W	M 4.515 (7,4) 24 W	U 4.50 24 W	M 3.992 (6,3) 0				
5	U (R) 4.90 (4,1) 0	U 4.50 24 W	U 4.90 (7,3) 104 IF	M 3.992 (6,5) 0	U (R) 4.50 104 IF			
6	U 4.90 (7.1) 64 IF	U (R) 4.90 (5,2) 0	M 3.992 24 W	U (R) 4.90 (4,3) 0	M 3.992 24 W	M 4.515 24 W		
7	U (R) 4.50 64 IF	M 4.515 24 W	U (R) 4.50 104 IF	M 4.515 24 W	U (R) 4.50 48 IF	U 4.20 (8,4) 0		
8	M 3.992 (3,6) 0	M 3.992 (8,2) 0	M 4.515 (7,2) 0	M 4.515 (8,3) 0				

- Fresh
- Once Burned
- Twice Burned
- Thrice Burned

LEU/MOX (Control Rod Location)
Enrichment (w/o Fissile)
Previous Location (Row, Column)
IFBA/WABA

Figure 20: Final Design of the Third Transition Cycle

	1	2	3	4	5	6	7	8
1	U (R) 0.860 0.909 38877							
2	U 1.136 1.253 167	M 1.253 1.470 20493						
3	U (R) 1.143 1.203 28640	U 1.213 1.305 18754	U (R) 1.125 1.182 28869					
4	U 1.107 1.210 164	M 1.044 1.180 22627	U 1.138 1.244 170	M 1.134 1.260 27376				
5	U (R) 1.124 1.179 28066	U 1.158 1.298 173	U 1.173 1.267 26077	M 1.203 1.380 25361	U (R) 1.265 1.332 192			
6	U 1.160 1.229 26334	U (R) 1.160 1.253 28077	M 1.348 1.440 204	U (R) 1.127 1.239 28297	M 1.228 1.422 188	M 0.945 1.298 145		
7	U (R) 1.147 1.334 172	M 1.177 1.418 178	U (R) 1.047 1.232 158	M 1.036 1.354 157	U (R) 0.781 1.120 119	U 0.324 0.715 36047		
8	M 0.528 0.840 27317	M 0.464 0.748 36887	M 0.525 0.878 25326	M 0.351 0.646 38420				

Assembly Type (CR Location)
Assembly Average Power
Assembly $F_{\Delta H}$
Assembly Average Burnup

Figure 21: Layout of Assembly Average Power, Radial Pin-peaking, and Assembly Average Burnup at BOC (150 MWD/MTM). (Assembly with hottest pin is shaded.)

	1	2	3	4	5	6	7	8
1	U (R) 0.939 0.961 48644							
2	U 1.313 1.384 13508	M 1.240 1.423 34023						
3	U (R) 1.145 1.191 41031	U 1.200 1.305 31771	U (R) 1.123 1.168 41102					
4	U 1.339 1.416 13510	M 1.170 1.293 34646	U 1.297 1.373 13439	M 1.056 1.194 39210				
5	U (R) 1.160 1.226 40453	U 1.337 1.406 13801	U 1.116 1.203 38444	M 1.054 1.184 37504	U (R) 1.260 1.370 14121			
6	U 1.103 1.144 38629	U (R) 1.110 1.176 38500	M 1.262 1.384 14198	U (R) 0.999 1.080 39650	M 1.111 1.303 12611	M 0.866 1.186 9706		
7	U (R) 1.158 1.333 12984	M 1.140 1.371 12777	U (R) 1.131 1.340 12234	M 0.981 1.253 10960	U (R) 0.771 1.065 8460	U 0.321 0.670 39469		
8	M 0.527 0.813 33071	M 0.469 0.723 42023	M 0.542 0.896 31221	M 0.358 0.647 42276				

Assembly Type (CR Location)
Assembly Average Power
Assembly $F_{\Delta H}$
Assembly Average Burnup

Figure 22: Layout of Assembly Average Power, Radial Pin-peaking, and Assembly Average Burnup at MOC (11,000 MWD/MTM). (Assembly with hottest pin is shaded.)

	1	2	3	4	5	6	7	8
1	U (R) 0.924 0.951 58650							
2	U 1.262 1.324 27436	M 1.151 1.295 46798						
3	U (R) 1.070 1.116 52959	U 1.133 1.232 44273	U (R) 1.071 1.115 52704					
4	U 1.310 1.392 27817	M 1.174 1.327 47197	U 1.274 1.364 27196	M 1.004 1.117 50092				
5	U (R) 1.098 1.154 52504	U 1.308 1.384 27891	U 1.079 1.156 50038	M 1.014 1.119 48394	U (R) 1.239 1.352 27355			
6	U 1.069 1.104 49909	U (R) 1.052 1.119 51583	M 1.250 1.369 27364	U (R) 0.996 1.064 50221	M 1.168 1.348 24648	M 0.964 1.303 19368		
7	U (R) 1.146 1.289 24975	M 1.156 1.403 24702	U (R) 1.154 1.325 24248	M 1.048 1.345 21640	U (R) 0.858 1.148 17077	U 0.387 0.733 43213		
8	M 0.560 0.835 38774	M 0.506 0.758 47085	M 0.587 0.940 37115	M 0.403 0.708 46262				

Assembly Type (CR Location)
Assembly Average Power
Assembly $F_{\Delta H}$
Assembly Average Burnup

Figure 23: Layout of Assembly Average Power, Radial Pin-peaking, and Assembly Average Burnup at EOC (21,564 MWD/MTM). (Assembly with hottest pin is shaded.)

ANALYSIS OF TRANSITION CYCLES

Virtually, the only difference of concern in this study between an all LEU core and a partial MOX core in global terms is purely neutronic. It is easily described by fast to thermal flux ratios. Higher ratios are associated with harder spectra, which is directly related to larger thermal and resonance-integral absorption cross sections as well as the energy distribution with which fission neutrons are born. Pu-239 is superior to U-235 in all these aspects. Therefore, the fast to thermal flux ratio is significantly higher in a partial MOX core than it is in an LEU core, as shown in Table V. The harder spectra affect many basic reactor parameters, including boron levels, reactivity coefficients and shutdown margin. These parameters along with peaking characteristics of the transition cores are discussed in this section.

TABLE V
Neutron Spectra Comparison³

Reactor Type	Fast to Thermal Flux Ratio		
	BOC	MOC	EOC
First Transition Cycle	8.43	7.69	6.65
Second Transition Cycle	9.80	8.65	7.40
Third Transition Cycle	10.39	9.12	7.78
LEU Core	7.12	-	6.13

Boron Levels

B-10 is worth less in partial-MOX cores than in LEU cores due to the harder spectrum in the former. This leads to much higher concentrations of soluble boron in the moderator, especially at BOC when the core is most reactive. It is not desired to

have high concentration levels of boron in the moderator, since moderator pH becomes a concern for plant systems, MTC at hot zero power (HZP) at BOC tends to become positive, and boron precipitation could hinder the coolant flow. In order to avoid high levels of soluble boron concentrations we used large numbers of burnable absorbers as shown in Table VI. Even though LEU cores use more IFBA-coated pins, partial-MOX transition cycles use a significant number of WABA rods. Each WABA rod contains roughly ten times the amount of boron found in an IFBA coating. As a result of using this large amount of burnable absorbers, boron levels became more reasonable throughout the cycles as shown in Figure 24. Figure 24 clearly shows that the higher the fraction of MOX in the core, the higher the boron concentration. For the LEU core, the boron letdown curve is somewhat flat over the first 3000 MWD/MTM, which is due to the fast depletion of B-10 in the IFBA coating. This is not the case in the partial-MOX cores since the spectrum is harder and most of the burnable absorbers are in the form of WABA rods which take longer to deplete.

TABLE VI
Burnable Absorber Loading Comparison

Burnable Absorber Type	LEU	First Transition Cycle	Second Transition Cycle	Third Transition Cycle
IFBA	6560	1984	1888	1888
WABA	0	1728	1440	1440

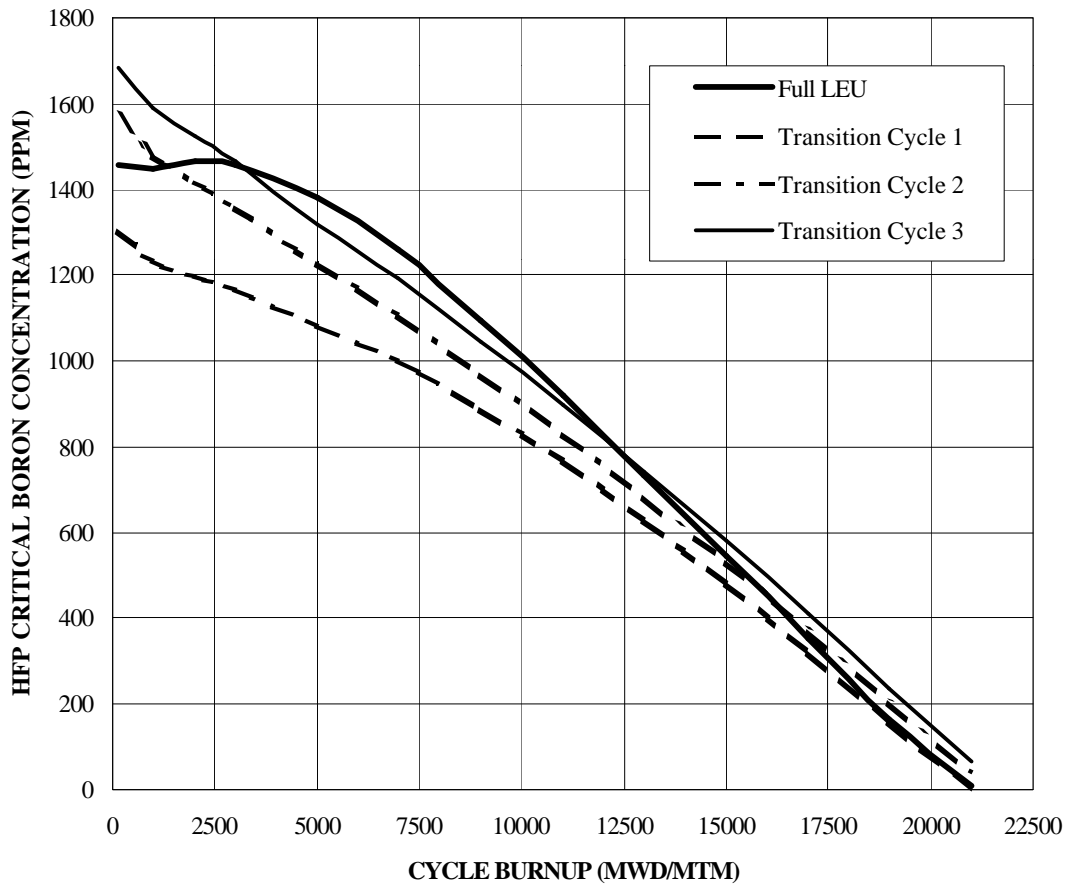


Figure 24: HFP Critical Boron Letdown Curves

In the case of a large break loss of coolant accident (LBLOCA), it is important to be able to shut the reactor down using soluble boron only, without taking any credit for the control rods at the core's most reactive condition, BOC. In this calculation no xenon and cold zero power (CZP) conditions apply, at which the moderator temperature is 68 °F and the primary system pressure is 14.7 psia, which are simply ambient conditions. The refueling water storage tank (RWST) is the source of the coolant with the high boron concentration levels. The boron concentration in the RWST is limited to under 2500 ppm due to pH concerns. When the reactor is to be shutdown in such a case, the water from the RWST mixes with the

primary system coolant. Thus, the post-LBLOCA boron concentration is a function of pre-LBLOCA levels. Figure 25 shows the correlation between the critical pre- and the achievable post-LBLOCA boron levels. For a pre-LBLOCA boron concentration, the post-LBLOCA boron concentration has to be on or below the line in Figure 25 for the shutdown to be achievable. Table VII lists the critical BOC equilibrium xenon HFP boron levels and the critical BOC CZP no xenon boron levels. The post-LBLOCA boron levels in this table fall below the line in Figure 25 for their respective pre-LBLOCA conditions, which ensures the shutdown capability of these transition cycles under LBLOCA severe conditions for all the cycles except the third transition cycle. This could be easily corrected by using enriched boron in the RWST.

TABLE VII
Critical Boron Concentration Comparison

Condition	LEU	First Transition Cycle	Second Transition Cycle	Third Transition Cycle
BOC, HFP, Equilibrium Xenon (ppm)	1458	1305	1576	1674
BOC, CZP, No xenon (ppm)	1782	1905	2193	2270

Reactivity Coefficients

Since boron is worth less in partial-MOX cores than in LEU cores, because of the harder spectrum in the former, the boron coefficient is less negative in partial-MOX cores as shown in Figure 26. The same fact affects the moderator temperature

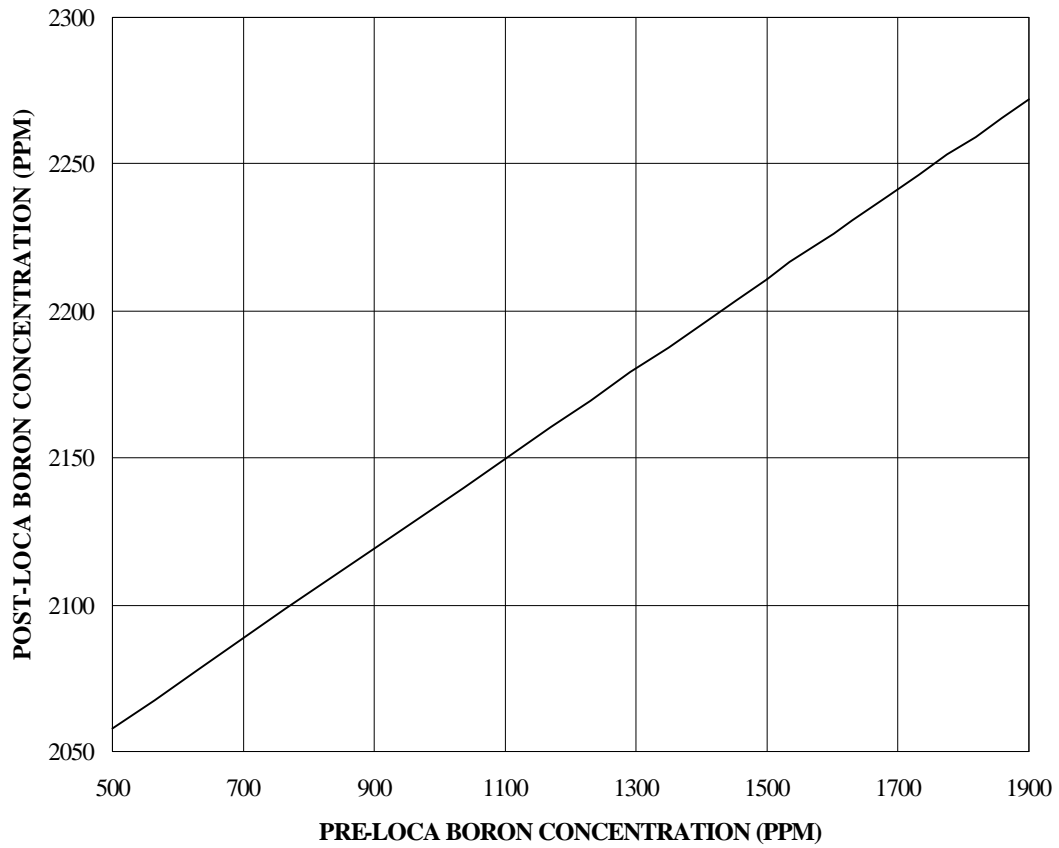


Figure 25: Post-LBLOCA Boron Concentration as a Function of Pre-LBLOCA Boron Concentration

coefficient (MTC) at BOC under no-xenon HZP conditions. MTC is limited to +7 pcm/^oF at these conditions. As Table VIII shows, MTC under these conditions is negative for the first and second transition cycles and slightly positive for the third transition cycle, yet less positive than typical LEU cores.

TABLE VIII
MTC Comparison at BOC, HZP, No Xenon Conditions

Parameter	LEU	First Transition Cycle	Second Transition Cycle	Third Transition Cycle
Critical Boron (ppm)	1955	1892	2238	2352
MTC (pcm/°F)	+4.37	-0.36	-0.37	+0.59

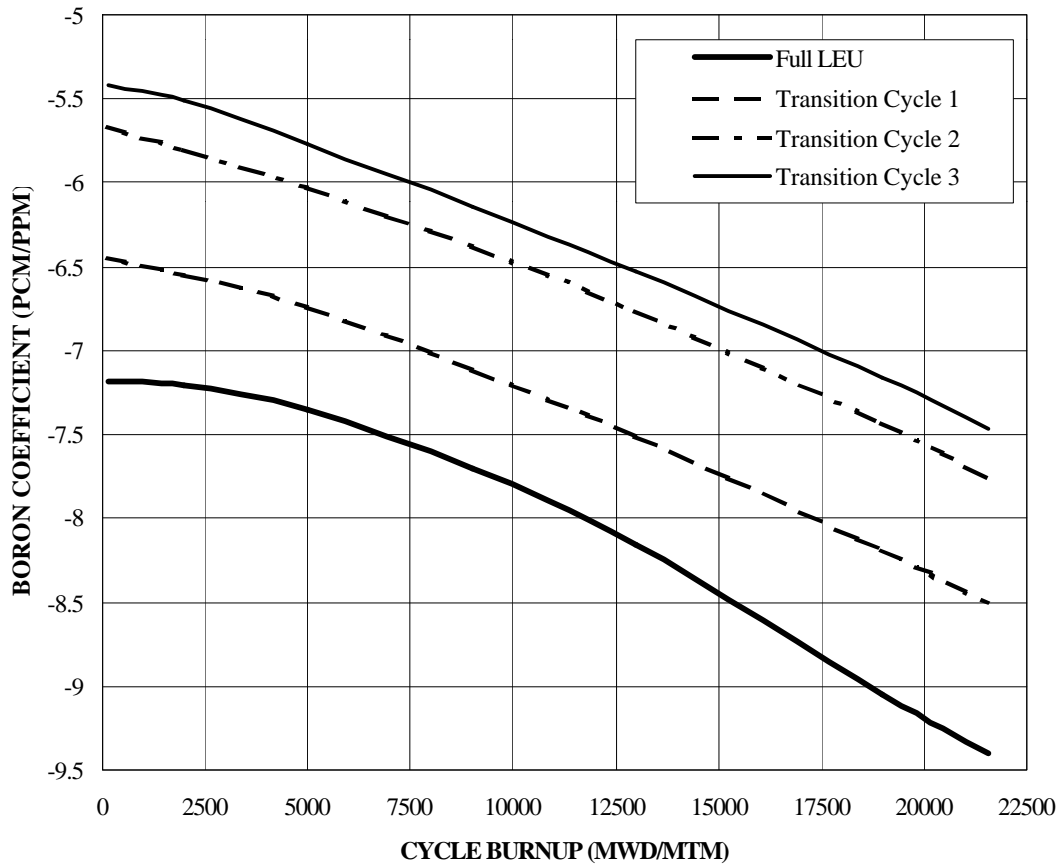


Figure 26: HFP Boron Coefficient vs. Burnup

As seen in Figure 27, moderator temperature coefficient tends to be more negative for a partial-MOX core than for an LEU core since the worth of soluble boron is significantly less, and the harder spectrum in the partial-MOX core makes it a more under-moderated core. At EOC, MTC for the three transition cores and a typical LEU core are almost identical because their spectra are comparable. (At this point in the cycle, a large fraction of the power in the LEU core is from fission of Pu-239, which is produced from parasitic absorptions in U-238: U-238 beta-decays to Np-239, which beta decays to Pu-239.)

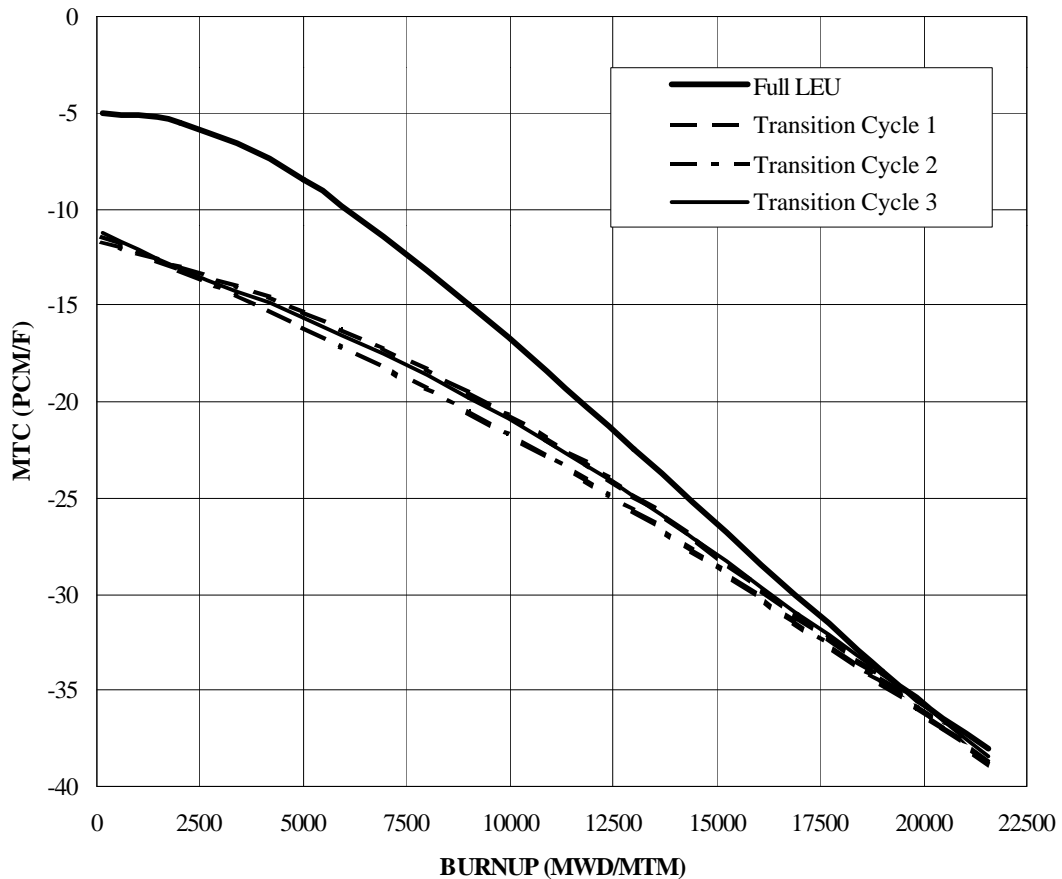


Figure 27: HFP MTC as a Function of Burnup

For safe operation, the total power coefficient (TPC) should be negative at all times throughout the cycle. Figure 28 presents TPC at BOC as a function of power. As expected, TPC at BOC is more negative for partial MOX cores than LEU cores. The difference in TPC between the several cores decreases with cycle burnup as the neutronic characteristics and the isotopic compositions of the cores becomes comparable. At EOC, TPC for the partial-MOX cores becomes comparable to that of an LEU core as shown in Figure 29.

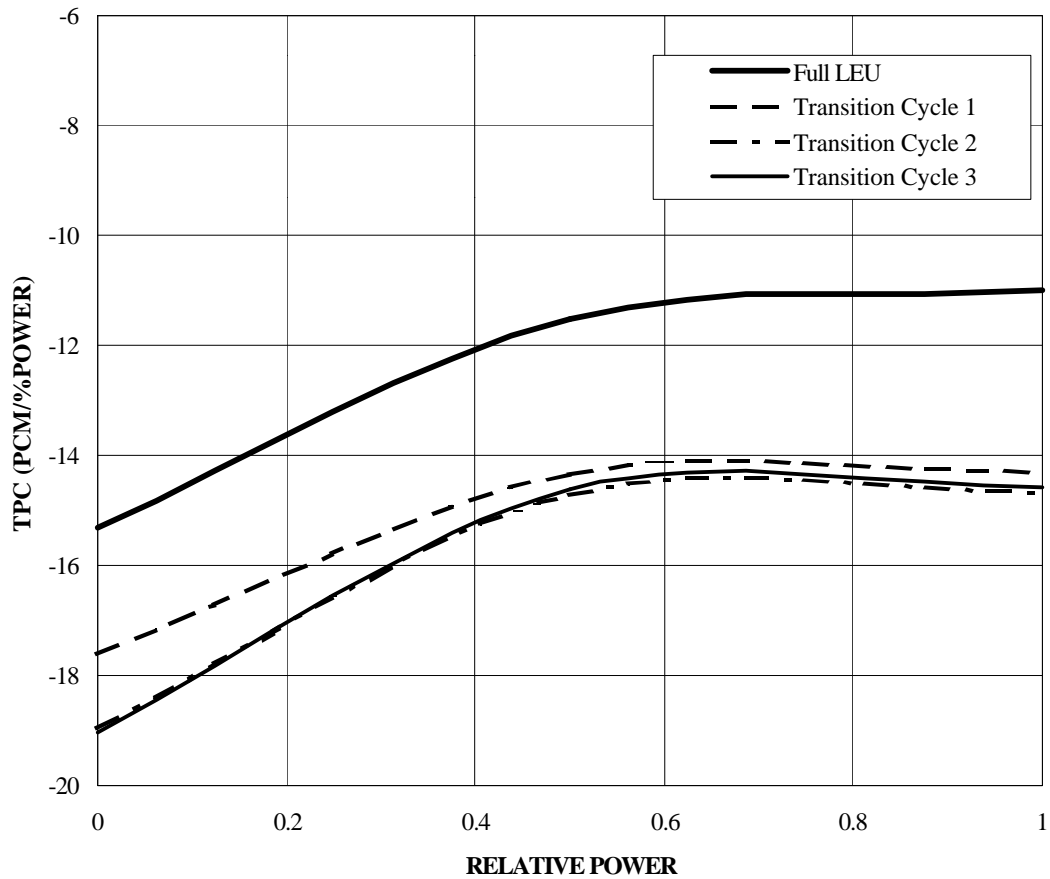


Figure 28: BOC TPC vs. Power

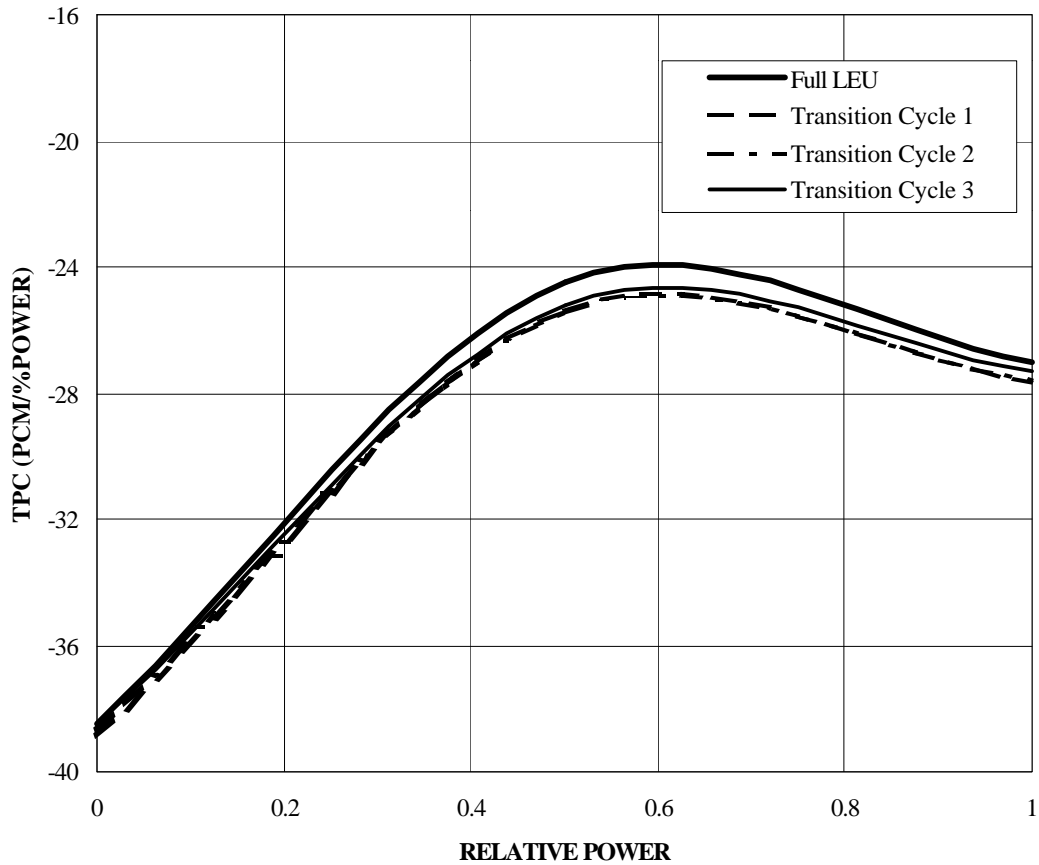


Figure 29: EOC TPC vs. Power

Power Peaking

Radial pin peaking, $F_{\Delta H}$, defined as the ratio of the integral of linear power along the rod with the highest integrated power to the average rod power,⁷ is one of the main parameters upon which we iterated during the transition cycles designs. The calculated design limit for $F_{\Delta H}$ is 1.528 for this specific plant. Our designs clearly remain under the design limit throughout the three transition cycles, as shown in Figure 30. The variability in peaking is mainly due to the shift in power distribution as burnable absorbers burn out.

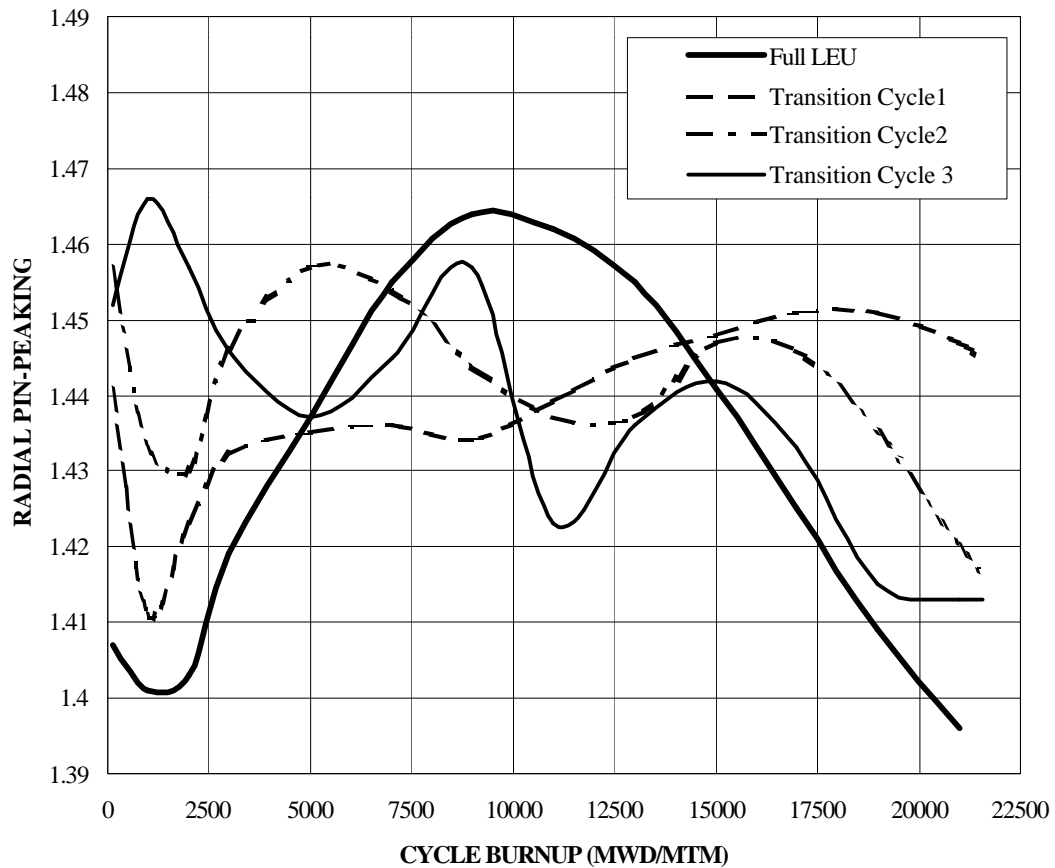


Figure 30: HFP Radial Pin-peaking vs. Burnup

Local power peaking, F_Q , which is defined as the maximum local fuel rod linear power density divided by the average fuel rod linear power density,⁷ clearly falls below the calculated design limit of 2.5 for this specific plant throughout the three transition cycles, as shown in Figure 31. In transition-core designs, we decreased F_Q by shaping the power axially, which we achieved by using part length WABA rods and IFBA coatings, which is common practice in LEU cores. We left approximately 9 inches at the bottom of the core and 6 inches at the top of the core without any burnable absorber.

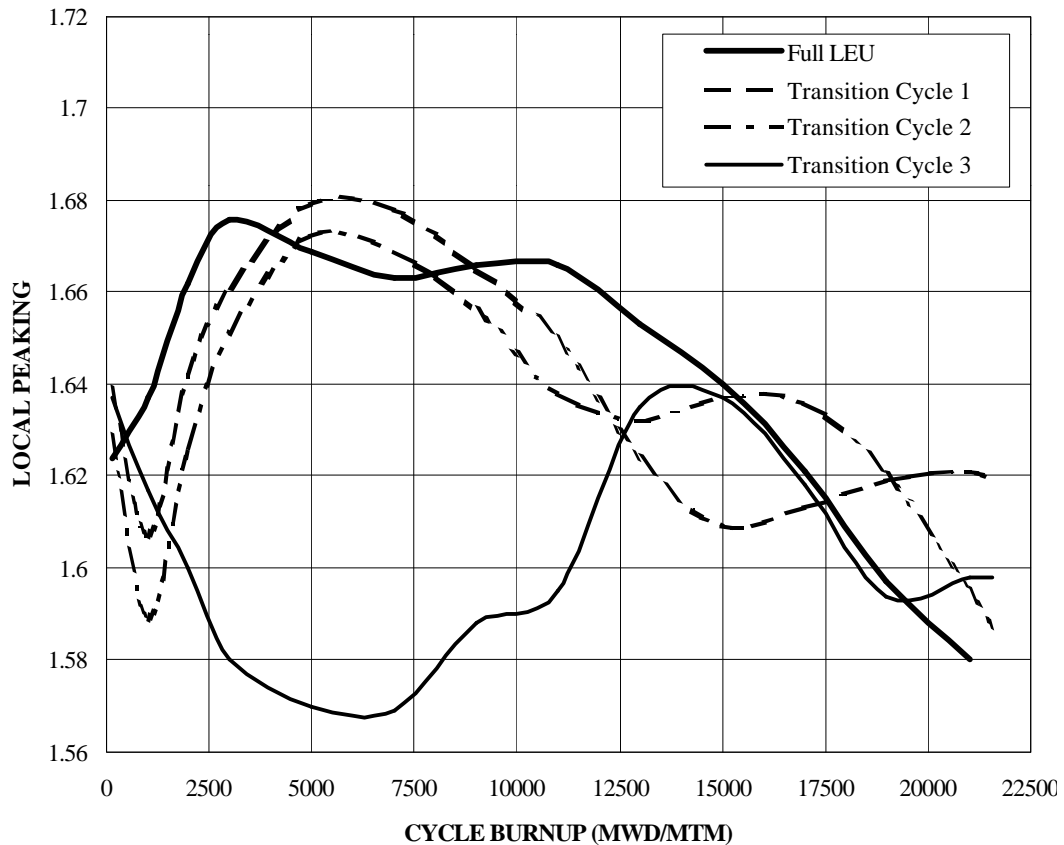


Figure 31: HFP Local Power Peaking vs. Burnup

Shutdown Margin (SDM)

Quite possibly the most limiting parameter in the total amount of MOX to be consumed in the core, with no design modifications in control rods, is shutdown margin (SDM). The harder spectrum in partial MOX cores decreases the worth of control rods. It is crucial to show that there is enough negative reactivity in the control rods to shut the reactor down at the worst and most difficult condition, at which the core reacts with the highest supply of positive reactivity. This condition is at EOC when the moderator temperature coefficient at its most negative. When the

reactor is shut down the temperature of the moderator drops more than 30 °F from HFP to HZP, thus adding a significant amount of positive reactivity which must be overcome by negative reactivity in the control rods. An extra precaution is taken by discarding the rod with the highest negative worth, assuming that it gets stuck out of the core. We also accounted for a few other allowances. First, moderator 6 °F deadband: we assumed that HFP temperature is 6 °F higher than predicted or HZP is 6 °F lower than predicted. Second, rod insertion allowance: during normal operation, partial insertion of some control rods is allowed to shape the radial and axial power distributions, so we assumed the maximum allowable insertion prior to shutdown. Third, voids: we assumed the existence of some voids around some fuel rods which would collapse right after shutdown. Table IX summarizes the SDM calculations and results for the three transition cycles. The first transition cycle had more SDM than a typical LEU core. The second and third transition cycles had just enough calculated SDM to slightly exceed requirements. The third transition cycle had 45.6 percent MOX fuel which is quite possibly the upper limit that the core could handle without any modifications in control rods.

The SDM calculated for the third transition cycle was fairly close to the limit. We could obtain a more comfortable margin by increasing control-rod worth. This could be achieved by using hybrid B₄C/Ag-In-Cd control rods instead of Ag-In-Cd control rods.

TABLE IX

EOC SDM Calculations

Parameter	LEU	First Transition Cycle	Second Transition Cycle	Third Transition Cycle
Number of Control Rods	53	53	53	53
Absorber Material	Ag-In-Cd	Ag-In-Cd	Ag-In-Cd	Ag-In-Cd
Worst Stuck Rod Location (Column, Row)	(1,2)	(1,2)	(3,3)	(3,3)
Core Percent MOX	0	14.5	33.2	45.6
CR Requirements (% $\Delta\rho$)				
Power Defect	2.84	2.87	2.87	2.90
Moderator 6 °F Deadband	0.24	0.24	0.24	0.24
Rod Insertion Allowance	0.50	0.50	0.50	0.50
Voids	0.05	0.05	0.05	0.05
(1) Total CR Requirement	3.63	3.66	3.66	3.69
Rod Worth (% $\Delta\rho$)				
All Rods In (ARI) Worth	7.10	7.22	6.51	6.64
(ARI - 1) Rod Worth	6.23	6.41	5.71	5.82
(2) (ARI - 1) - 10%	5.61	5.77	5.14	5.24
Shutdown Margin (% $\Delta\rho$)				
SDM [(2) - (1)]	1.98	2.11	1.48	1.55
SDM Requirement	1.30	1.30	1.30	1.30
Excess SDM	0.68	0.81	0.18	0.25

SUMMARY

We were able to design the first three transition cycles taking a four-loop Westinghouse reactor from a full LEU core to one with 45 percent MOX. Our calculations indicate that our designs meet all neutronic limits, and that the partial-MOX cores would behave much like LEU cores. The most limiting parameter appears to be EOC SDM.

CHAPTER V

SUMMARY AND CONCLUSIONS

In this study, we successfully presented three transition-cycle designs from an all LEU core to a partial-MOX core with a final MOX fraction of 45.6 percent. The transition-cycle designs involved the development of weapons-grade MOX assemblies for which the enrichment distribution was optimized for peaking purposes using three different enrichments per assembly and four total different enrichments. We used Vogtle Plant Unit 1 as a model four-loop reactor in its technical description and operation limitations and regulations.

All the transition cycles met the important regulatory and operational limits of an LEU core including peaking characteristics, boron levels, reactivity coefficients, and shutdown margins. Table X is a summary of the design parameters of the three transition cycles compared to a typical LEU cycle. This unit is capable of consuming 0.462 MT of WGPu a year. So, if several similar units are used, the disposition objective can be accomplished in a relatively short period of time. Pu-240 abundance reaches 20 percent at burnups around 30,000 MWD/MTM.⁷ The average discharge burnup of MOX assemblies at the end of the third transition cycle is 47,477 MWD/MTM. Consequently, the spent fuel will have low weapons utility. Shutdown margins for the second and third transition cycles are somewhat tight, but they can be improved upon by using hybrid B₄C/Ag-In-Cd control rods which have increased negative worth.

The reactor-analysis computer codes we used in these designs, namely CASMO-3, PHOENIX-P and ANC, have not been benchmarked for weapon-grade MOX fuel analysis. Some benchmarking of PHOENIX-P and ANC was done with

reactor-grade MOX but without burnable absorbers. These two codes are used for design and analysis of European partial-reactor-grade-MOX cores at the Beznau plant in Sweden. However, the MOX assemblies used in Beznau have relatively low enrichments and they do not use burnable absorbers. Thus, there is some lack of confidence in the results from CASMO-3 and PHOENIX-P, especially around steep power and flux gradients near WABA rods and inserted control rods. This directly affects the SDM calculation, since PHOENIX-P generates cross sections with control rods inserted.

There is still a significant amount of work to be done before we can declare that these cycle designs are operable in real cores. Safety analyses need to be performed including some transient analysis such as rod ejection and steamline break. Prior to any further work with these cycle designs, the design and analysis codes need to be benchmarked for weapons-grade assemblies with discrete burnable absorbers present. Nevertheless, we are confident that our designs, or very similar ones, could in fact be used in a PWR-based disposition program.

TABLE X
Summary of Design Parameters

Design Parameter	LEU	First Transition Cycle	Second Transition Cycle	Third Transition Cycle
LEU Feed Assemblies	84	64	48	48
MOX Feed Assemblies	0	28	36	36
Excess SDM (% $\Delta\rho$)	0.68	0.81	0.18	0.25
Feed Loading (MTM)				
LEU	35.5	27.0	20.3	20.3
MOX	0	11.8	15.2	15.2
Core Total Loading (MTM)	82.6	81.6	81.6	81.6
Feed Enrichment (w/o fissile)				
LEU	4.20, 4.50	4.20, 4.50	4.90	4.50
MOX		4.52, 3.99	4.52, 3.99	4.52, 3.99
Average WGPu w/o in Feed Region	0	4.56	4.56	4.56
Total WGPu (MTM) in Feed Region	0	0.540	0.693	0.693
Total WGPu (MTM) Used per Reactor Year	0	0.360	0.462	0.462
Cycle Length (MWD/MTM)	20,750	21,564	21,564	21,564
Cycle Length (EFPD)	481	493	493	493
B-10 abundance (a/o)	19.8	19.8	19.8	19.8
Burnable Absorbers Loading				
IFBA	6560	1984	1888	1888
WABA	0	1728	1440	1440

REFERENCES

1. "Technical Summary Report for Surplus Weapons-Usable Plutonium Disposition," United States Department of Energy, Office of Fissile Material Disposition (17 July 1996).
2. "Management and Disposition of Excess Weapons Plutonium," National Academy of Sciences, Committee on International Security and Arms Control (1994).
3. "Plutonium Disposition in Existing Pressurized Water Reactors," Westinghouse Electric Corporation (1 June 1994).
4. "CASMO-3, User's Manual," STUDSVIK of America, Inc.
5. "PHOENIX-P, User's Manual," Westinghouse Electric Corporation.
6. "ANC, User's Manual," Westinghouse Electric Corporation.
7. DEBDAS BISWAS, ROY W. RATHBUN, SI YOUNG LEE, and MELVIN R. BUCKNER, "Weapons-Grade Plutonium Disposition in Pressurized Water Reactors," *Nuclear Science and Engineering*, **121**, 1 (1995).
8. "Weapons-Grade Plutonium Dispositioning, Volume 1, Executive Summary," Idaho National Engineering Laboratory (June 1993).

9. "Weapons-Grade Plutonium Dispositioning, Volume 2, Comparison of Plutonium Disposition Options," Idaho National Engineering Laboratory (June 1993).
10. "Weapons-Grade Plutonium Dispositioning, Volume 3, A new Reactor Concept Without Uranium or Thorium for Burning Weapons-Grade Plutonium," Idaho National Engineering Laboratory (June 1993).
11. "Weapons-Grade Plutonium Dispositioning, Volume 4, Plutonium Dispositioning in Light Water Reactors," Idaho National Engineering Laboratory (June 1993).
12. RICHARD D. ANKNEY AND DEBDAS BISWAS, "Weapons-Grade Plutonium Disposition in Existing Westinghouse PWRs," *Trans. Am. Nucl. Soc.*, **71**, 488 (1994).
13. "U.S. Department of Energy Plutonium Disposition Study Phase II, Volume II, Technical Review Committee Report," United States Department of Energy, Office of Fissile Materials Disposition (April 1995).
14. "Summary Report of the Screening Process to Determine Reasonable Alternatives for Storage and Disposition of Weapons-Usable Fissile Materials," Office of Fissile Materials Disposition (14 February 1995).
15. Fissile Materials Disposition, <http://web.fie.com/htdoc/fed/doe/fsl/pub/menu/any/>.

VITA

Abdelhalim Ali Alsaed was born on 11 September 1971 in Tulkarm, Palestine. He graduated from Omar Ben El-Khatib high school in Baqua El-Sharquia in 1990. He received his Bachelor of Science degree in Nuclear Engineering from Texas A&M University in May of 1994. He can be reached at: Department of Nuclear Engineering, Texas A&M University, College Station, Texas 77843-3133.